NBS-GCR-86-510

A Model for Vertical Wall Fire in A Stratified Atmosphere

A.K. Kulkarni
J. Hwang

March 1986

Sponsored by
U.S. DEPARTMENT OF COMMERCE
National Bureau of Standards
Center for Fire Research
Gaithersburg, MD 20899

NBS-GCR-86-510

A MODEL FOR VERTICAL WALL FIRE IN A STRATIFIED ATMOSPHERE

A.K. Kulkarni
J. Hwang

Pennsylvania State University
Department of Mechanical Engineering
University Park, PA 16802

March 1986

Grant Number 60NANB4D0037

Sponsored by
U.S. DEPARTMENT OF COMMERCE
National Bureau of Standards
Center for Fire Research
Gaithersburg, MD 20899

Notice

This report was prepared for the Center for Fire Research of the National Engineering Laboratory, National Bureau of Standards under Grant Number 60NANB4D0037. The statements and conclusions contained in this report are those of the authors and do not necessarily reflect the views of the National Bureau of Standards or the Center for Fire Research.

A Model for Vertical Wall Fire in a Stratified Atmosphere

by

Anil K. Kulkarni
Assistant Professor

and

Jen-Jyh Hwang
Graduate Assistant

Department of Mechanical Engineering
The Pennsylvania State University
University Park, PA 16802

ANNUAL REPORT

on Grant No. 60NANB4D0037 for the period of 8/15/84 to 8/14/85

submitted to

Center for Fire Research
National Bureau of Standards
Gaithersburg, MD 20899

ABSTRACT

A comprehensive mathematical model is presented for understanding the characteristics of a burning vertical wall immersed in a quiescent ambient atmosphere having a nonuniform vertical distribution of temperature and oxidizer mass fraction. Such a stratified atmosphere occurs, for example, in the interior of a room or aircraft cabin on fire. A set of partial differential equations and suitable boundary conditions describing a laminar flow of exothermically reacting species is solved using the Keller Box finite difference scheme. Results of burning rate and flow parameters (such as the maximum vertical velocity, flame position, etc.) are presented for many different cases of stratified atmosphere. A comparison of these results with the results for the nonstratified atmosphere shows that the predicated burning rate for a thermally stratified case behaves like a linear combination of results for the corresponding nonstratified cases; however, this does not hold for compositionwise stratified atmosphere. The stratification has a substantial nonlinear effect on the flow strucure in the wall fire. Different possibilities for surface reradiation models are also discussed.

TABLE OF CONTENTS

I. INTRODUCTION

This report summarizes the progress made during the period August 15, 1984 to August 14, 1985, on the project entitled, "A Model for Vertical Wall Fire in a Stratified Atmosphere," under grant number 60NANB4D0037.

The overall objective of this investigation is to achieve more understanding of characteristics of a burning vertical wall immersed in a stratified ambient atmosphere through mathematical modelling.

In a typical compartment fire, two clearly distinguishable layers appear in the compartment interior in the form of hot, oxidizer-lean gases on the top of fresh, cold incoming air. A relatively steep vertical gradient of temperature and composition separates the two layers [1]. This situation has been observed in room fires, corridor fires and aircraft cabin fires [2-4]. A burning vertical wall can be strongly affected by the stratification of the interior atmosphere because the wall fire flow is usually a strongly buoyant, natural convection flow, and the buoyancy itself depends on the difference between the temperatures of the ambient atmosphere and the fire plume. Consequently the burning characteristics of surrounding walls and the overall fire scenario are influenced by the stratification inside the room.

There are several boundary layer models of vertical wall fire available in the literature which deal with different aspects of the fire, such as the radiation, flame spread, turbulence, chemical reaction rates, etc. [5-11]. However, this is the first comprehensive mathematical model for a natural convection vertical wall fire which takes into account the effect of stratified ambient atmosphere.

The specific objectives of this project were: (1) to develop a boundary layer model of a vertical wall fire in a thermally and compositionwise stratified ambient atmosphere; (2) to develop a computer code to solve the model numerically; (3) to obtain numerical results for various types of atmospheric stratification; and (4) to compare the results with nonstratified cases as well as any available pertinent experimental data from the literature.

Following sections present details of the model, numerical solution procedure, comparison of results, and conclusions.

A list of publications, supported by the grant and developed during the past year on this project, is given below.

1. Kulkarni, A.K., H.R. Jacobs, and J.J. Hwang. Natural Convection Over an Isothermal Vertical Surface Immersed in a Thermally Stratified Fluid. Presented at the National Heat Transfer Conference, Denver, CO, August 1985. Paper No. 85-HT-40. Submitted to the International Journal for Heat and Mass Transfer.

2. Kulkarni, A.K., J.J. Hwang. Free Convection Vertical Wall Fire in Various Types of Stratified Ambient Atmosphere. Accepted for presentation at the AIAA 24th Aerospace Sciences Meeting, January 1986.

3. Kulkarni, A.K., J.J. Hwang. A Model for a Burning Vertical Wall in the Stratified Atmosphere of a Compartment Fire. Presented at the 1985 Fall Technical Meeting, Eastern Section of the Combustion Institute, November 1985.

II. THE MATHEMATICAL MODEL

2.1 Physical Description

The mathematical model attempts to simulate overall characteristics of a burning vertical wall which is a part of a compartment as depicted in Figure 1. The wall fire is assumed to be a buoyancy driven boundary layer flow of chemically reacting gases. The energy released by chemical reactions in the fire is partly convected to the wall, convected upward, and radiated by the hot gases. At the wall, there is an energy balance of convection from the boundary layer, conduction to the interior of the wall, reradiation by the wall surface, radiation received from the gases, and heat needed to pyrolyze the fuel in the wall. The gaseous fuel is then convected and diffused in the boundary layer where it mixes with the oxidizer from the atmosphere. The chemical reaction between the fuel and oxidizer releases energy which makes the flow buoyant and thus the process continues.

The presence of a nonuniform surrounding atmosphere adds complexities to the problem. An opening in a compartment, such as a door, provides fresh air from the bottom while the hot combustion gases mixed with air exit from the top of the opening. This creates stratification of the compartment atmosphere in the form of hot and oxidizer-lean gases on the top and cold, oxidizer-rich air in the lower portion. The stratification affects the wall fire in mainly three ways. The upward buoyancy force, which drives the natural convection boundary layer flow, depends on the

temperature of the ambient atmosphere, and the outer edge conditions for the temperature and the gas composition are also altered.

2.2 Governing Equations and Boundary Conditions

The physical processes described above are cast into the following set of governing equations and boundary conditions. Although most fires are turbulent in nature, a laminar flow approximation is expected to reveal a significant insight into basic mechanisms and interesting features of the problem while allowing considerable ease in the numerical solution. The flow is assumed to be steady with known conditions of stratification. The conservation equations are:

Continuity:
$$\frac{\partial}{\partial x}(\rho u) + \frac{\partial}{\partial y}(\rho v) = 0 \qquad (1)$$

Momentum:
$$\rho u \frac{\partial u}{\partial x} + \rho v \frac{\partial u}{\partial y} = \frac{\partial}{\partial y}\left(\mu \frac{\partial u}{\partial y}\right) + g\left(\rho_\infty - \rho\right) \qquad (2)$$

Energy:
$$\rho u \frac{\partial h_T}{\partial x} + \rho v \frac{\partial h_T}{\partial y} = \frac{\partial}{\partial y}\left(\rho \alpha \frac{\partial h_T}{\partial y}\right) + \dot{q}_c''' + \dot{q}_R''' \qquad (3)$$

Species:
$$\rho u \frac{\partial Y_i}{\partial x} + \rho v \frac{\partial Y_i}{\partial y} = \frac{\partial}{\partial y}\left(\rho D \frac{\partial Y_i}{\partial y}\right) + \dot{m}_i''' \quad ; \qquad (4)$$

$$i = F(\text{fuel}),\ O(\text{oxidizer})$$

The boundary conditions are:

At $y = 0 : u = 0, \quad T = T_w$ (5)

At $y \to \infty : u = 0, \; Y_F = 0$ (6)

$Y_O = Y_{O\infty}(x)$; a prescribed function

$T = T_\infty(x)$; a prescribed function

Mass transfer balance at the surface:

$$0 = (\rho v)_w Y_O - (\rho D)_w \frac{\partial Y_O}{\partial y} \tag{7}$$

$$\dot{m}''_w Y_{FP} = (\rho v)_w Y_{FP} = (\rho v)_w Y_F - \rho D \frac{\partial Y_F}{\partial y}$$

Heat transfer balance at the surface:

$$k_g \left(\frac{\partial T}{\partial y}\right)_{gas} = \dot{m}''_w h_p + \dot{q}''_{R,w} - \dot{q}''_{R,g} \tag{8}$$

The buoyancy term is modeled using the ideal gas law. For combustion, the thin flame sheet model is used [5] which assumes that the flame is diffusion controlled, i.e., the rate of chemical reactions is infinite compared to the diffusion of fuel and oxidizer species. This assumption is quite accurate for the prediction of the mass burning rate and most other parameters as long as the combustion conditions are not very close to the extinction conditions, based on our prior experience [10]. The transport coefficients $\rho\mu$, ρk, and $\rho^2 D$ are assumed to be constant. For the gas phase

radiation loss, optically thin gas assumption is made which is quite reasonable for a small, laminar fire. Even for somewhat larger fires, this assumption will not affect the results critically, unless $\dot{q}_R'''$ is relatively large compared to other terms in the energy equation. Further, the gas phase radiation is assumed to be equally split between the fraction lost to the ambient atmosphere and the fraction incident upon the burning wall. The reradiation from the burning wall surface to the ambient atmosphere needs careful consideration because of the shape factor determined by the ambient atmosphere (having nonconstant $T_\infty(x)$) with respect to a given location on the burning wall, and it is discussed later. The value of the heat of pyrolysis used here includes the energy loss in the wall by conduction.

2.3 Transformation

The governing equations and boundary conditions were recast into a nondimensional and incompressible form using the following transformation.

$$s = x/H \tag{9}$$

$$\eta = C_1 \, x^{-1/4} \int_0^y \frac{\rho}{\rho_r} \, dy \tag{10}$$

$$\text{where, } C_1 = (g/\nu^2_r)^{1/4} \tag{11}$$

$$\beta_{FO} = Y_F - \{[Y_O - Y_{O\infty}(x)]/\nu_s\} \tag{12}$$

$$\beta_{FT} = Y_F + \{[h-h_\infty(x)]/h_c\} \tag{13}$$

A stream function, ψ, is introduced in order to automatically satisfy the continuity equation.

$$\psi = 4\, C_2\, \nu_r\, s^{3/4}\, f(s,\eta) \tag{14}$$

where,
$$C_2 = (C_1 H^{3/4})/4 \tag{15}$$

such that,

$$\rho u = \rho_r \frac{\partial \psi}{\partial y} \qquad \text{and} \qquad \rho v = -\rho_r \frac{\partial \psi}{\partial x} \tag{16}$$

The governing equations then take the following form.

$$\frac{\partial^3 f}{\partial \eta^3} + \frac{3}{4} f \frac{\partial^2 f}{\partial \eta^2} - \frac{1}{2}\left(\frac{\partial f}{\partial \eta}\right)^2 = s\left(\frac{\partial f}{\partial \eta}\frac{\partial^2 f}{\partial \eta \partial s} - \frac{\partial^2 f}{\partial s^2}\frac{\partial f}{\partial s}\right) - \frac{h_c}{\bar{C}_p T_\infty}\left(\beta_{FT} - Y_F\right) \tag{17}$$

$$\frac{1}{Pr}\frac{\partial^2 \beta_{FT}}{\partial \eta^2} + \frac{3}{4} f \frac{\partial \beta_{FT}}{\partial \eta} = s\left(\frac{\partial f}{\partial \eta}\frac{\partial \beta_{FT}}{\partial s} - \frac{\partial \beta_{FT}}{\partial \eta}\frac{\partial f}{\partial s}\right) + \frac{Hs}{h_c}\frac{\partial f}{\partial \eta}\left[\bar{C}_p \frac{\partial T_\infty}{\partial x}\right] + \frac{4\bar{K}_p \sigma}{h_c}\left(\frac{Hs}{g}\right)^{1/2} \frac{T^5}{\rho_\infty T_\infty} \tag{18}$$

$$\frac{1}{Sc}\frac{\partial^2 \beta_{FO}}{\partial \eta^2} + \frac{3}{4} f \frac{\partial \beta_{FO}}{\partial \eta} = s\left(\frac{\partial f}{\partial \eta}\frac{\partial \beta_{FO}}{\partial s} - \frac{\partial \beta_{FO}}{\partial \eta}\frac{\partial f}{\partial s}\right)$$

$$- \frac{Hs}{\nu_s}\frac{\partial f}{\partial \eta}\frac{\partial Y_{O\infty}}{\partial x} \qquad (19)$$

The boundary conditions are transformed as follows.

At $\eta=0$:

$$\frac{\partial f}{\partial \eta} = 0 \qquad (20)$$

$$\beta_{FT} - Y_F = \frac{\bar{C}_p}{h_c}(T_w - T_\infty)$$

$$\frac{\partial \beta_{FT}}{\partial \eta} = Sc\left\{\frac{3}{4} f + s\frac{\partial f}{\partial s}\right\}\left\{Y_{F,P} - Y_F\right\} - \frac{h_p Pr}{h_c}\left\{\frac{3}{4} f + s\frac{\partial f}{\partial s}\right\}$$

$$+ \frac{Pr}{h_c \rho_r}\left\{\frac{Hs}{g\nu_r^2}\right\}^{1/4} \varepsilon\,\sigma\,(T_w^4 - T_\infty^4)$$

$$- \frac{Pr}{h_c \rho_r}\left(\frac{Hs}{g}\right)^{1/2}\left\{2\,\varepsilon\,\bar{K}_p\,\sigma \int_0^\infty \frac{\rho_r}{\rho} T^4 d\eta\right\}$$

$$\frac{\partial \beta_{FO}}{\partial \eta} = Sc\left\{\frac{3}{4} f + s\frac{\partial f}{\partial s}\right\}\left\{Y_{F,P} - \beta_{FO} + Y_{O\infty}/\nu_s\right\}$$

At $\eta=\infty$:

$$\frac{\partial f}{\partial \eta} = \beta_{FT} = \beta_{FO} = 0 \qquad (21)$$

III. NUMERICAL SOLUTION

3.1 General Procedure

The governing equations presented above form a set of three partial differential equations which are nonlinear, third order, coupled, and nonhomogeneous with nonconstant boundary conditions. In order to obtain a numerical solution for this set, a modified Keller Box finite difference method was used [12]. The equations were first transformed by defining additional, dependent variables as follows.

$$U = \frac{\partial f}{\partial \eta} \tag{22}$$

$$V = \frac{\partial^2 f}{\partial \eta^2} \tag{23}$$

$$P = \frac{\partial \beta_{FT}}{\partial \eta} \tag{24}$$

$$R = \frac{\partial \beta_{FO}}{\partial \eta} \tag{25}$$

After substituting the above variables in the governing equations, a set of seven, first order, coupled, differential equations was obtained. The equations were then converted into finite difference form. Equations [22-25] were written for the nodes (n, j-1/2), and the remaining governing equations were written for the nodes (n-1/2, j-1/2), using a central difference scheme. (Refer to Figure 2). Here, all the variables at (n-1)st step were known; at the nth step, they were unknown. Nonlinear terms were quasilinearized based on the first two terms in Taylor's series.

Further solution involved setting up a corresponding coefficient matrix for the seven equations and the boundary conditions for the linearized system of equations. The coefficient matrix was composed of blocks of seven coefficients each. This matrix, along with the matrix for nonhomogeneous terms, were then solved using the block-tridiagonal-elimination method.

Reasons for adopting the Keller Box method were:

a) Second order accuracy with arbitrary (nonuniform) spacing in x and y directions
b) Capability of handling rapid x variation, which is expected due to an abrupt change in the ambient temperature caused by hot and cold layers
c) Easy programming of a large number of coupled equations.

3.2 Computer Program Checks

Before embarking on the task of solving the seventh order mathematical model, we solved two similar but simpler models using the same method. These models were intended to familiarize us with the Keller Box method and to help us look for difficult spots in the more complex seventh order problem; they were described in our second quarterly progress report.

In order to verify the accuracy of the final computer code, three major checks were made: (a) numerical errors in balancing various terms in the equations; (b) comparison of results with known calculations available in the literature for nonstratified conditions; and (c) an extreme

condition for a stratified case for which the solution is intuitively obvious. They are described in the following.

The equations were solved progressively from the leading edge to the top of the wall at preselected values of x/H. After the equations were solved at any particular height, some arbitrary points in the boundary layer were selected at that height and the balance of mass, momentum, and energy was checked. The relative magnitude of the residue (i.e. the left hand side minus the right hand side of a finite difference equation divided by the largest term) is plotted in Figure 3a as a function of the normalized height for three governing equations of β_{FT}, β_{FO} and f. The maximum error or imbalance among all the equations is less than 0.4%. Corrections in boundary conditions as a function of the iteration count are shown in Figure 3b at three different heights. It was found that after 3 to 4 iterations the corrections were down to practically zero. These and other numerical error checks confirmed the accuracy of the numerical scheme.

Figure 4 shows comparison of our numerical solution with finite difference solution of Sibulkin, et al. [7] and integral solution of Kim, et al. [5]. It may be noted that the ordinate scale is amplified for an easy comparison. The figure shows the variation of burning rate of a vertical plate of Polymethylmethacrylate (PMMA) under nonstratified conditions with ambient temperatures of 25°C and 200°C (constant with respect to height). The differences between our solution and those of References 5 and 7 are very small.

In the third set of computer program checks, results were obtained for three cases: $T_\infty(x) = 25^oC$; $T_\infty(x) = 200^oC$; and with $T_\infty(x)$ nonconstant (stratified case) as shown in Figure 5. In the stratified case, the $T_\infty(x)$ was held constant (25^oC) for x/H from 0.0 to 0.00067, linear from 25^oC to 200^oC for x/H from 0.00067 to 0.0067, and then constant at 200^oC up to x/H equal to 1.0. This means that the ambient temperature was perturbed very close to the leading edge. The calculated dimensionless burning rate started out at that for 25^oC, then it was perturbed, but soon it reached a constant value, same as that for the $T_\infty=200^oC$ case. Since almost all of the wall is immersed in an atmosphere with $T_\infty=200^oC$, except for $0<x/H<0.0067$, the burning rate is expected to approach to that for the isothermal atmosphere case. In other words, a disturbance near the leading edge is expected to smooth out as the boundary layer grows. Our solution indeed predicts this behavior.

The above three types of checks gave us confidence in the capability of the computer code for predicting behavior of a wall fire in a stratified medium.

IV. RESULTS AND DISCUSSION

4.1 General

Results were obtained for several types of stratified cases with both $T_\infty(x)$ and $Y_{O\infty}(x)$ varying. Properties of polymethylmethacrylate were used for the solid fuel wall characteristics. The wall temperature was assumed to be constant at 660 K and the total wall height was fixed at 15 cm for calculation purposes. Table 1 shows constants used in the computer program. Results are presented in four major sections (i) a typical (base) case of thermal stratification; (ii) various other types of thermal stratification, (iii) stratification in oxidizer mass fraction and (iv) surface reradiation models.

4.2 A Base Case for Thermal Stratification

A typical profile of the ambient atmosphere temperature in a compartment fire was first selected as the base case as shown in Figure 6. This stratification model was derived based on measured data in a room fire experiment with certain openings [13]. The temperature $T_\infty(x)$ is assumed to be constant at 25°C for the first 40% of the total wall height. Then it linearly increases to 60% of the height, and then it remains constant at 200°C to the top of the wall. The ambient oxidizer mass fraction, $Y_{O\infty}$, is assumed to remain constant throughout at 0.233. The base case is compared with two other nonstratified cases, one with $T_\infty(x)=25^oC$ (constant from x=0 to H) and other with $T_\infty(x)=200^oC$ (constant from x=0 to H).

Figure 7 shows the dimensionless maximum upward velocity in the fire ($u_{max}/\sqrt{gx}$) as a function of the normalized height for the stratified and nonstratified cases. The velocity for the stratified case is initially the same as that for T_∞=25°C case as expected, then it gradually slows down toward the value for T_∞=200°C case. It never reaches to that of the T_∞=200°C case, probably because of the high momentum of gases in the lower portion of the boundary layer. The broken line shows the predicted variation of velocity between $0.4<x/H<0.6$ assuming a linear superposition of results from the T_∞=25°C and T_∞=200°C (nonstratified) cases. It is clearly seen that we cannot simply superpose results for T_∞=constant cases to derive results for the stratified case. The dimensionless shear stress and the convective heat flux to the wall shown in Figures 8 and 9 behave in a similar manner. The flame sheet moves away from the wall in the stratified case with increasing height because of the increasing $T_\infty(x)$, as seen in Figure 10. It too remains well within the two limiting cases of nonstratified atmosphere and carries with it the effect of the lower T_∞ in the bottom layer into the top layer having a higher T_∞.

Figure 11 shows the variation of the dimensionless burning rate (proportional to $\dot{m}''x^{1/4}$) as a function of the height for the three cases of ambient temperature variation. The burning rate for the stratified case shoots above that of the T_∞=200°C case for a short distance and then slowly drops down. The overshoot is probably caused by the particular boundary reradiation model used here; this point will be discussed in detail later. In general, burning characteristics of the wall are expected to be influenced by the upward momentum of the boundary layer gases, the flame

temperature, the flame sheet distance from the wall, and the radiation loss from the boundary layer; all of which are affected due to the stratification. Variation of the dimensional burning rate is shown in Figure 12. Considering the highly expanded scale of the ordinate in Figure 11, and from the results in Figure 12, we conclude that the burning rate prediction is not far from that obtained by assuming linear superposition of the nonstratified cases (shown by broken line). Later, it will be evident that the linear superposition is a reasonably good approximation for the burning rate in the case of the thermal stratification only, not for the oxidizer concentration stratification.

Figures 13 and 14 show isothermal contours and streamlines, respectively, for the present case of stratification. The isotherms clearly show the effect of the ambient temperature stratification on the temperature distribution inside the boundary layer. A careful examination of streamlines in Figure 14 reveals a slight bulging of the boundary layer as it enters the upper, higher T_∞, region. It must be noted here that the boundary layer assumption in the governing equations is not quite valid in the outer region of the boundary layer near the interface of the upper and lower layers where there are non-negligible gradients in streamwise direction. However, this region is relatively small with respect to the remaining flow domain and is not likely to affect the overall characteristics of the burning wall very significantly.

4.3 Other Types of Thermal Stratification

In addition to the base case stratification discussed above, two other types of thermal stratification were considered and their results were compared to the base case. As shown in Figure 15, we consider a "step" stratification where the two layers are separated by a very steep temperature gradient at the middle height of the wall, and a linear stratification where $T_\infty(x)$ varies continuously from the bottom to the top of the wall.

Figures 16-19 show the maximum vertical velocity in the boundary layer, the shear stress, the convective heat transfer to the wall, and the flame position (all dimensionless) as a function of the height for the three cases. A linear superposition of results from nonstratified cases of T_∞=25°C and T_∞=200°C (not shown here) would be a reasonable approximation for the linear stratification, but not for the step stratification. When the base case is compared with the step stratification it is clear that the effects of specific variation of $T_\infty(x)$ are carried for a short distance and then diminish downstream. Again, it must be noted that particularly for the step stratification, the boundary layer assumption is not quite valid at the height where there is the sharp gradient in $T_\infty(x)$. However, this is restricted to a small region and its influence is expected to reduce rapidly as the flow continues downstream.

Variation of the dimensional burning rate with height is shown in Figure 20. Again the sharp rise and overshoot for the step stratification case is, we feel, due to the specific surface radiation model used; it is discussed further in section 4.5. In general, the burning rate for

the continuous stratification and the step stratification behaves like a linear combination of nonstratified cases, except for a local overshoot when there is a sudden change in $T_\infty(x)$.

4.4 Effect of Ambient Oxidizer Mass Fraction Varying With Height

Results for three cases are presented: $Y_{O\infty}$ constant at 0.233; $Y_{O\infty}$ constant at 0.200; and , $Y_{O\infty}(x)$ linearly decreasing from 0.233 at x/H=0.4 to 0.200 at x/H=0.6 and constant otherwise (see Figure 21). In all three cases a $T_\infty(x)$ variation same as the base case (shown in Figure 6) was assumed and hence the first of the three cases is identical to the base case discussed in section 4.2.

Figures 22-25 show variation of the maximum vertical velocity, wall shear stress, convective heat flux, and flame position with respect to the height. Results for the stratified case are relatively closer to the $Y_{O\infty}$=0.233 (constant) case than the $Y_{O\infty}$=0.200 (constant) case for all the parameters except for the convective heat transfer. This indicates that the upstream effect is very strong on the distribution of the oxidizer mass fraction inside the boundary layer. In general, it is concluded that a simple superposition of results for the nonstratified cases (compositionwise) is not sufficient to predict the results for the stratified case.

The dimensional burning rate and the flame temperature results are shown in Figures 26 and 27. Once again we confirm that in the case of the oxidizer mass fraction stratification, a linear combination of

results from nonstratified cases does not make accurate predictions. Thus the behavior of the wall fire for the thermally stratified case substantially differs from the compositionwise stratified case.

4.5 Surface Reradiation Models

In all the results presented so far, it was assumed that the radiation heat loss by the (isothermal) burning wall was given by:

$$\dot{q}''_{R,W} = \varepsilon \sigma \{T_W^4 - T_\infty^4(x)\}$$

When there is a sudden change in $T_\infty(x)$, this model causes a sudden change in the burning rate as seen in Figure 20. Note that T_W is always held constant. In reality the wall would loose energy by radiation to both the upper and lower layers at every location and the relative magnitude of the energy loss to each layer would depend on the nature of the ambient atmosphere (assuming that the flame thickness is small and it remains optically thin). Therefore, in addition to the above model two other models were considered: the wall radiates equally to the upper layer and the lower layer at every location (Model B); and the radiation loss increases continuously and linearly from the bottom to the top (Model C). The thermal stratification was the same as that used in the base case (Figure 6). Specifically the boundary radiation models are expressed as:

Model A: $$\dot{q}''_{R,W} = \varepsilon \sigma \left(T_W^4 - T_\infty^4(x)\right) \qquad (26)$$

Model B: $$\dot{q}''_{R,W} = 0.5\ \varepsilon\ \sigma\ (T_w^4 - T_\infty^4(0)) + 0.5\ \varepsilon\ \sigma\ (T_w^4 - T_\infty^4(H)) \quad (27)$$

Model C: $$\dot{q}''_{R,W} = \left(1 - \frac{x}{H}\right)\ \varepsilon\ \sigma\ (T_w^4 - T_\infty^4(o)) + \frac{x}{H}\ \varepsilon\ \sigma\ (T_w^4 - T_\infty^4(H)) \quad (28)$$

Figure 28 shows the dimensional burning rate variation with the height using the three models. The sharp variation of burning rate using model A is not evident in the results using models B and C. For models A and C the burning rates at x/H=0 and x/H=1 are almost the same. This is expected because the surface radiation loss at these two extreme positions is the same for the two models. For model B, the surface radiation loss is constant irrespective of the stratification and therefore it is higher at x/H=0 and lower at x/H=1 compared to the other two models, as expected. Figure 29 shows variation of the dimensionless maximum upward velocity with height using the three models and for two nonstratified cases T_∞=25°C and T_∞=200°C. The models do not seem to affect the maximum velocity significantly. We are continuing to explore these and other surface reradiation models to determine which of these is the most appropriate one.

V. SUMMARY AND CONCLUSIONS

A comprehensive mathematical model has been developed for studying characteristics of a burning vertical wall immersed in a stratified ambient atmosphere. The important features of the model are: (a) buoyancy term dependent on the prescribed $T_\infty(x)$; (b) boundary conditions keyed to the prescribed $T_\infty(x)$ and $Y_{O\infty}(x)$; and (c) the inclusion of surface and flame radiation. The governing equations are solved using Keller Box finite

difference method and results are presented for several cases of stratification. Major conclusions of this study are as follows.

1. Flow characteristics (for example, the maximum upward velocity) are significantly affected by the stratification and they differ substantially from the results obtained by a simple linear combination of results for the nonstratified cases.

2. Burning rate results for thermally stratified cases are reasonably close to the linear superposition of results for nonstratified cases; this does not hold true for stratifed atmosphere with a nonuniform ambient oxidizer mass fraction.

3. Surface reradiation models should be checked carefully for predicting the burning rate of a burning wall in a stratified atmosphere.

We wish to gratefully aknowledge the support of the Center for Fire Research, National Bureau of Standards, through Grant No. 60NANB4D0037 for conducting this work.

Table 1 - Constants used in calculations

$\bar{C}_p$ = 1.3 kJ/kg K

h_c = 26560 kJ/kg

h_p = 1590 kJ/kg

Pr = 0.7

Sc = 0.7

T_W = 660 K

$Y_{F,P}$ = 1.0

ε = 0.9

ν_r = 59.55×10^{-6} m^2/s

ν_s = 1.918

ρ_r = 0.5235 kg/m^3

Nomenclature

$\bar{C}_p$ - mean specific heat

C_1, C_2 - constants, Eqs. (11) and (15)

D - binary mass diffusivity

f - dimensionless stream function, Eq. (14)

g - acceleration due to gravity

H - height of wall

h_c - heat of combustion

h_p - heat of pyrolysis

h_T - thermal enthalpy

K - thermal conductivity

K_p - Planck mean absorption coefficient

$\dot{m}'''$ - volumetric mass generation rate

P - defined variable, Eq. (24)

Pr - Prandtl number

$\dot{q}''_{R,g}$ - gas radiation to the wall

$\dot{q}''_{R,w}$ - surface radiation loss

$\dot{q}'''_{c}$ - volumetric heat generation

$\dot{q}'''_{R}$ - volumetric gas radiation loss

R - defined variable, Eq. (25)

s - dimensionless height, Eq. (9)

Sc - Schmidt number

T - Temperature

U - defined variable, Eq. (22)

V - defined variable, Eq. (23)

u - velocity parallel to wall

v - velocity normal to wall

x - distance along wall

y - distance normal to wall

Y - species mass fraction

$Y_{F,P}$ - fuel mass fraction at solid wall

α - thermal diffusivity

β_{FO} - transformed variable, Eq. (12)

β_{FT} - transformed variable, Eq. (13)

ε - wall emissivity

η - dimensionless distance, Eq. (10)

μ - dynamic viscosity

ν - kinematic viscosity

ν_s - stoichiometric coefficient

ρ - density

ψ - stream function

σ - Stephan-Boltzmann constant

Subscripts

F - fuel

g - gas phase

O - oxygen

r - reference

w - wall

∞ - ambient atmosphere

References

1. Quintiere, J.G., "A Perspective on Compartment Fire Growth," Combustion Science and Technology, Vol. 39, p. 11, 1984.

2. Zukoski, E.E., "Development of a Stratified Ceiling Layer in the Early Stages of a Closed-Room Fire," Fire and Materials, Vol. 2, No. 2, p. 54, 1978.

3. Cooper, L.Y., Harkleroad, M. Quintiere, J.G., Rinkinen, W., "An Experimental Study of Upper Hot Layer Stratification in Full Scale Multiroom Fire Scenarios," Journal of Heat Transfer, p. 741, Vol. 104, 1982.

4. Delichatsios, M.A., "Modeling of Air- craft Cabin Fires," (Factory Mutual Corporation), National Bureau of Standards Report No. NBS-CGR-84-473, 1984.

5. Kosdon, F., Williams, F.A. and Buman, C., "Combustion of Vertical Cellulosic Cylinders in Air," Twelfth Symposium (International) on Combustion, p. 253, The Combustion Institute, Pittsburgh, PA, 1969.

6. Kim, J.S., deRis, J. and Kroesser, F.W., "Laminar Free Convective Burning of Fuel Surfaces," Thirteenth Symposium (International) on Combustion, p.949, The Combustion Institute, Pittsburgh, PA, 1971.

7. Sibulkin, M., Kulkarni, A.K. and Annamalai, K., "Effects of Radiation on the Burning of Vertical Fuel Surfaces,"Eighteenth Symposium (Interantional) on Combustion, p. 611, The Combustion Institute, 1980.

8. Fernandez-Pello, A.C., "Flame Spread Modeling," Combustion Science and Technology, Vol. 39, p. 119, 1984.

9. Ahmad, T., and Faeth, G.M., "Turbulent Wall Fires," Seventeenth Symposium (International) on Combustion, p. 1149, The Combustion Institute, Pittsburgh, PA, 1978.

10. Sibulkin, M., A.K. Kulkarni, and K. Annamalai. Burning on a Vertical Fuel Surface with Finite Chemical Reaction Rate. Combustion and Flame 44, p. 187, 1982.

11. Chen, C.H. and T'ien, J.S., "Fire Plume Along Vertical Surfaces: Effect of Finite-Rate Chemical Reactions," 21st National Heat Transfer Conference, Seattle, WA, July 24-28, 1983.

12. Cebeci, T. and Bradshaw, P., Physical and Computational Aspects of Convective Heat Transfer, Springer-Verlag, New York 1984.

13. Quintiere J.G., Rinkinen, W.J., and Jones, W.W., "The Effect of Room Openings on Fire Plume Experiment," Combustion Science and Technology, Vol. 26, p. 193, 1981.

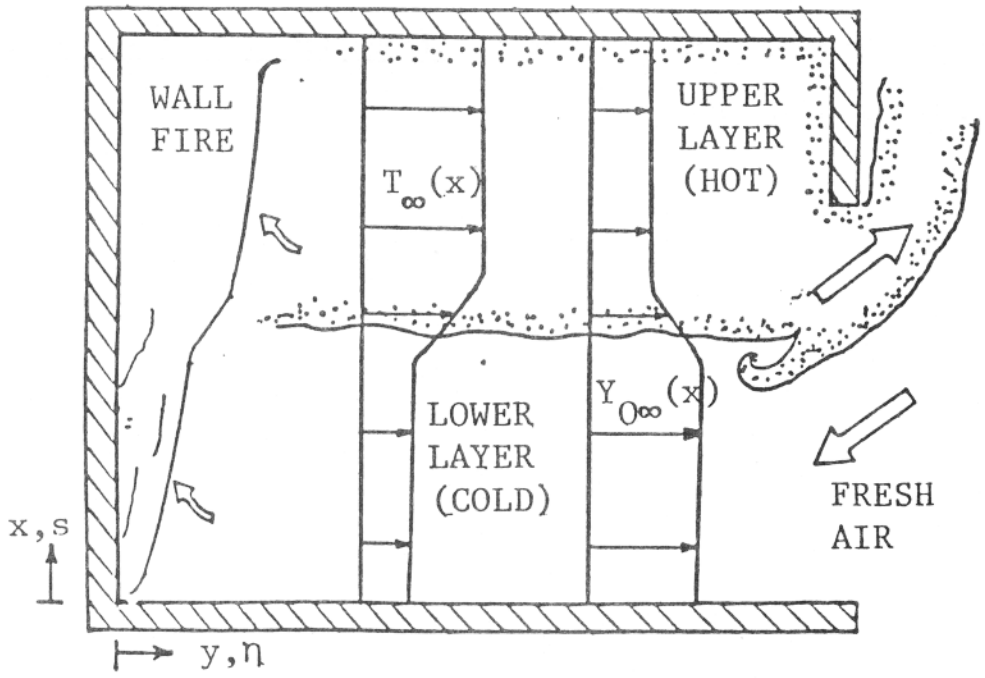

Figure 1 ; A schematic of a vertical wall fire in a stably stratified atmosphere of a compartment with an open door.

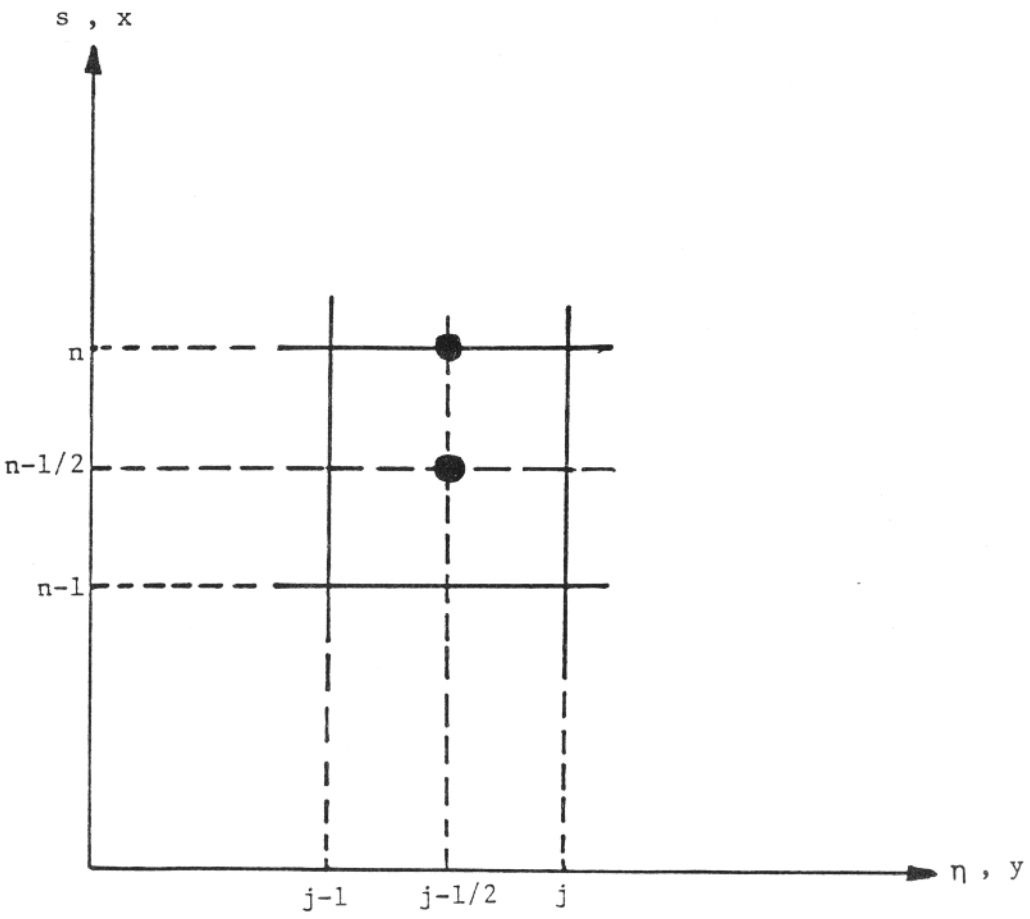

Figure 2 : Grid pattern for numerical solution.

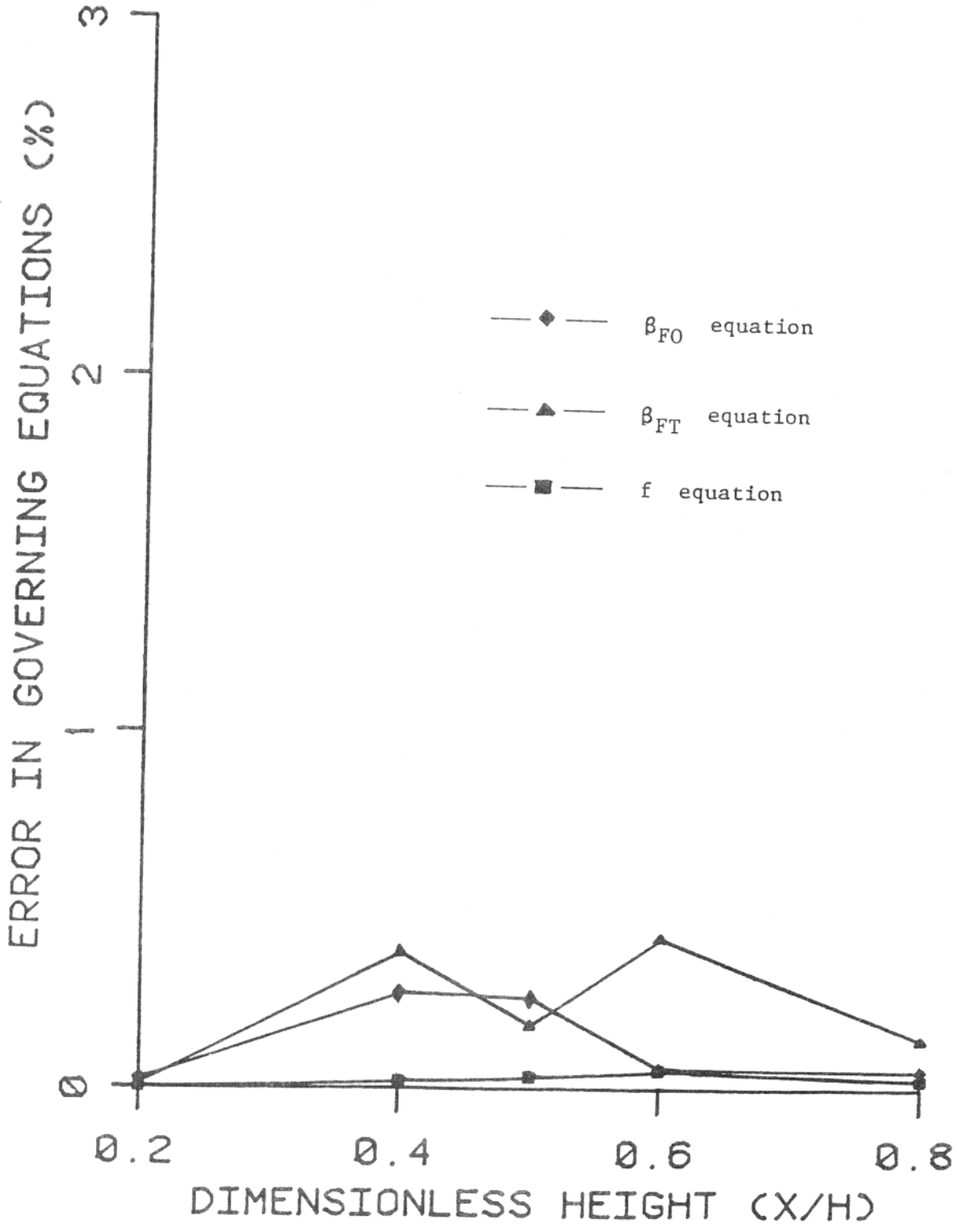

Figure 3a : Residual errors in governing equations at a node near the flame position.

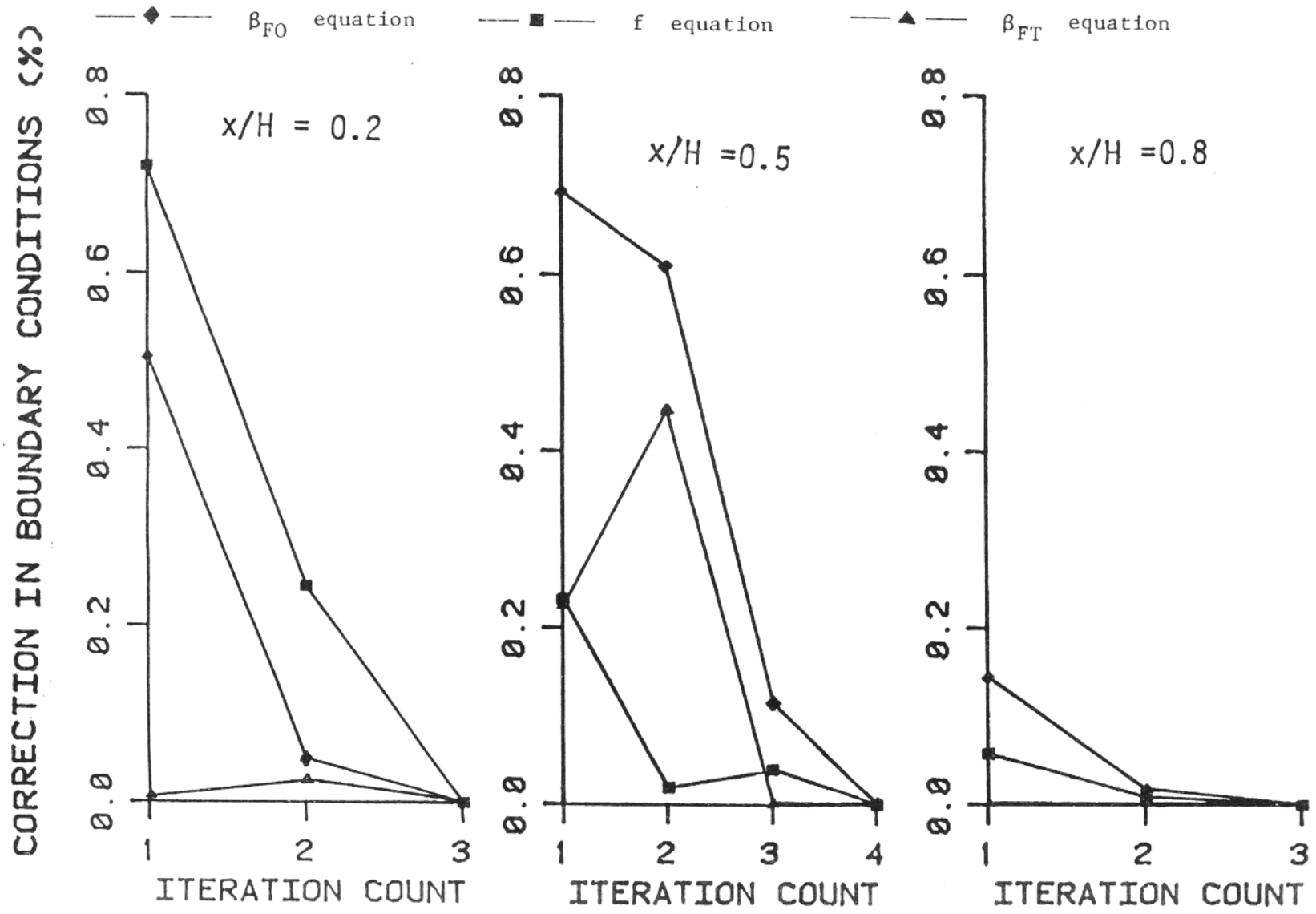

Figure 3b : Correction in boundary conditions at three vertical locations.

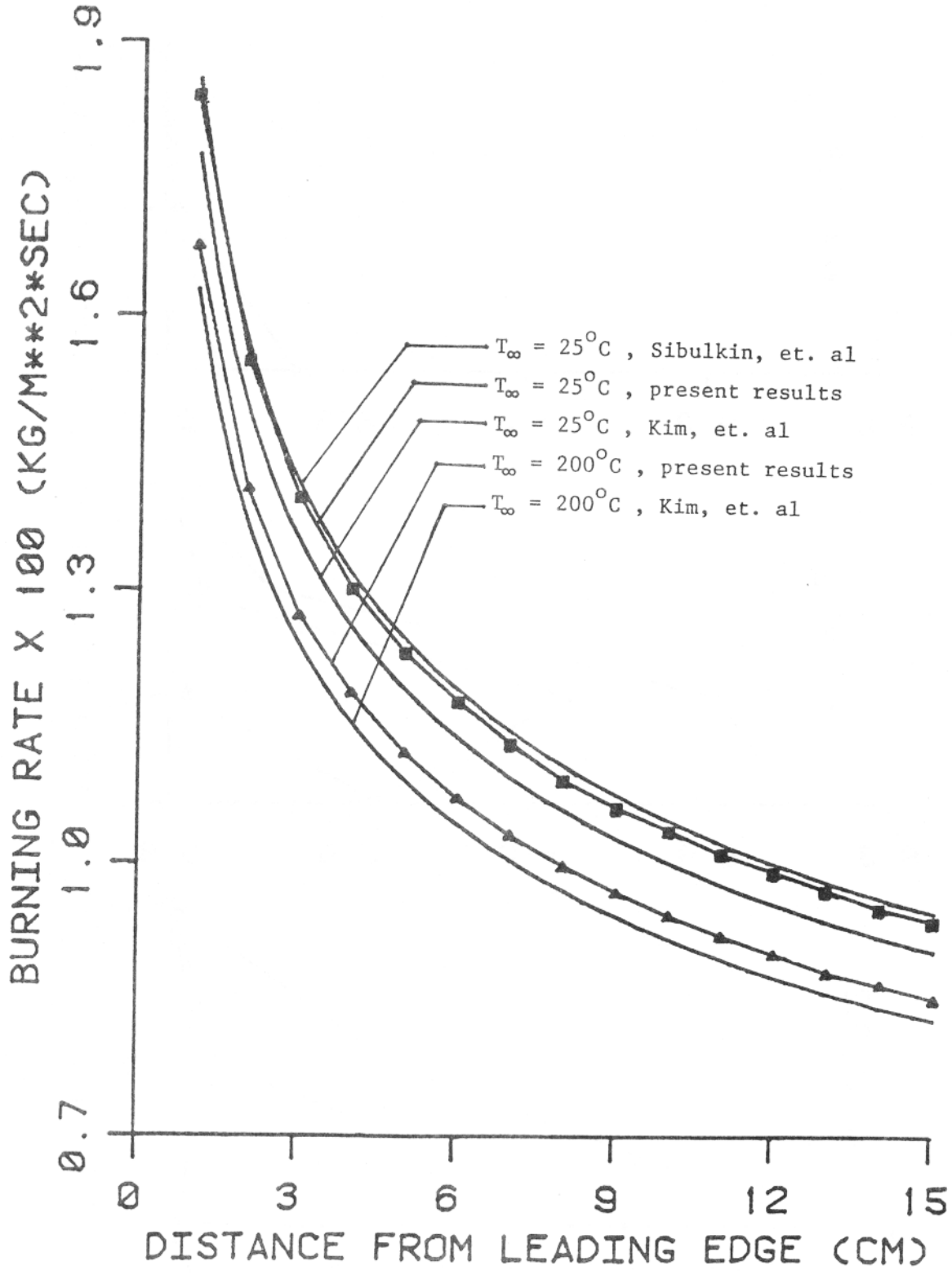

Figure 4 : Comparison of present resluts with some available results in the literature for ambient atmosphere having a uniform temperature.

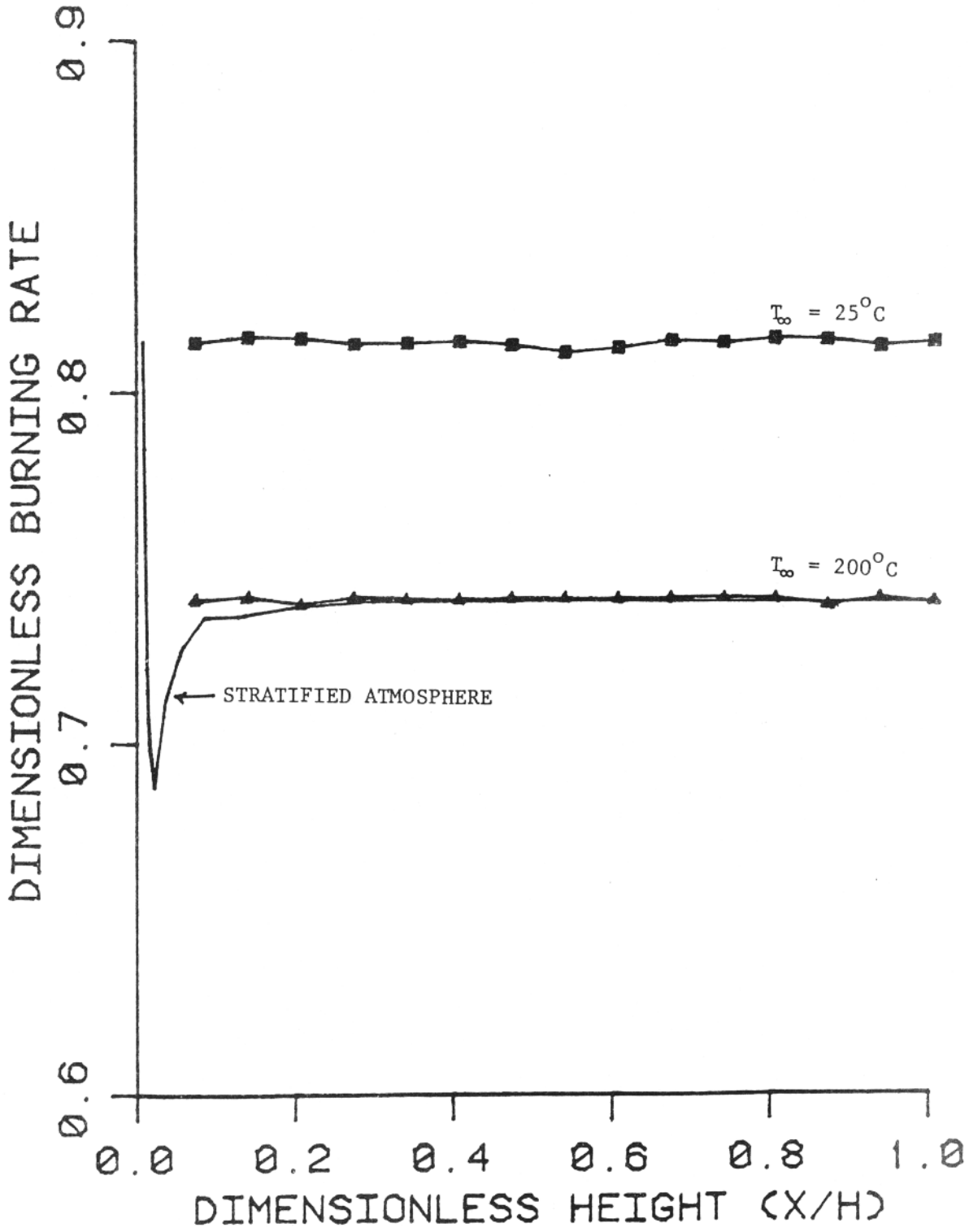

Figure 5 : Comparison of results for two cases of constant T_∞ and one case of stratified atmosphere with $T_\infty(x)$ varying very close to the leading edge only.

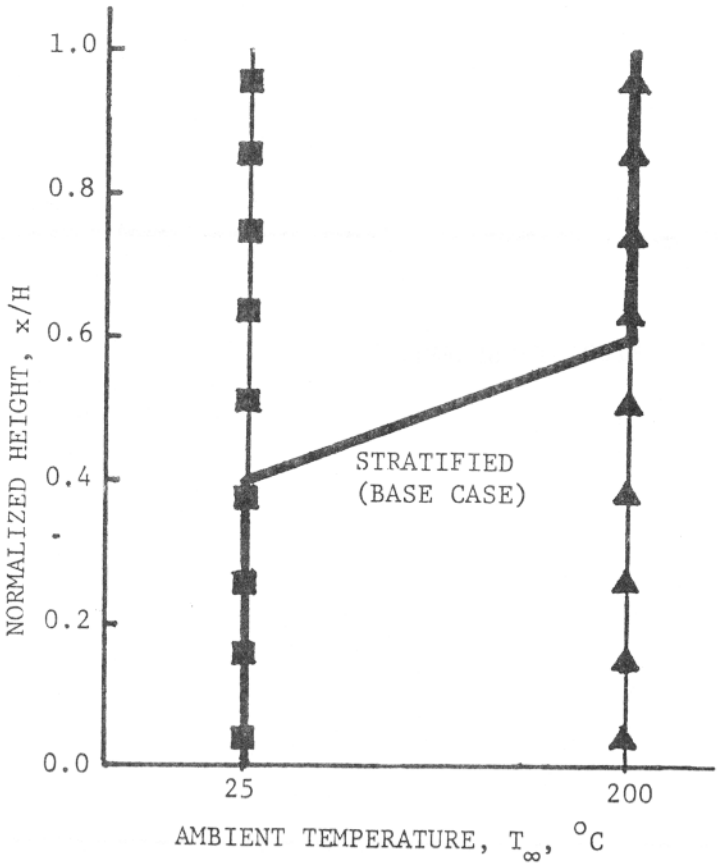

Figure 6 : A typical case of thermal stratification (the base case) is shown (——) along with two cases of nonstratified atmosphere : T_∞ = 25°C (—■—) and T_∞ = 200°C (—▲—).

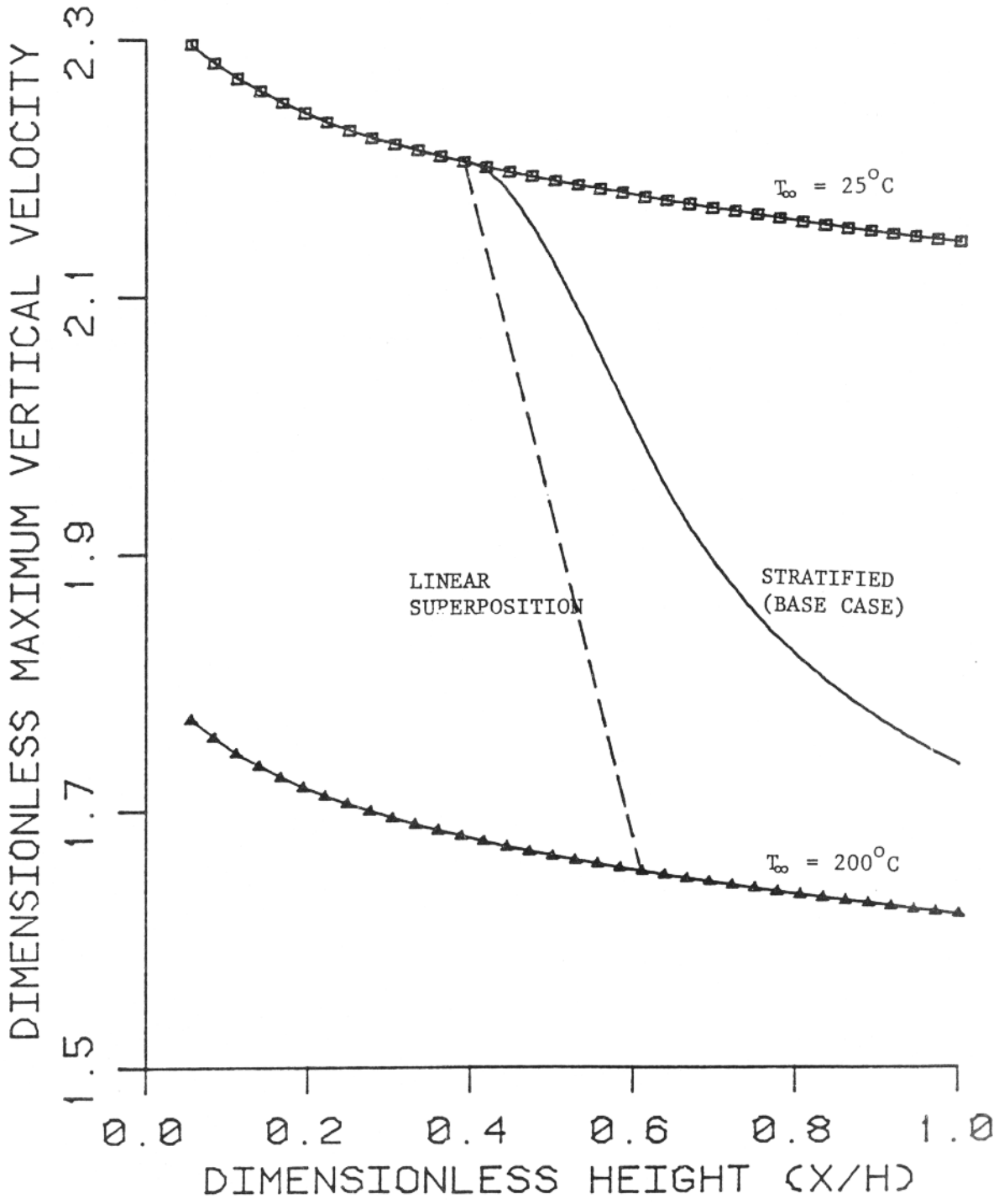

Figure 7 : Dimensionless maximum upward velocity against normalized height for the base case of stratified atmosphere and two other nonstratified cases.

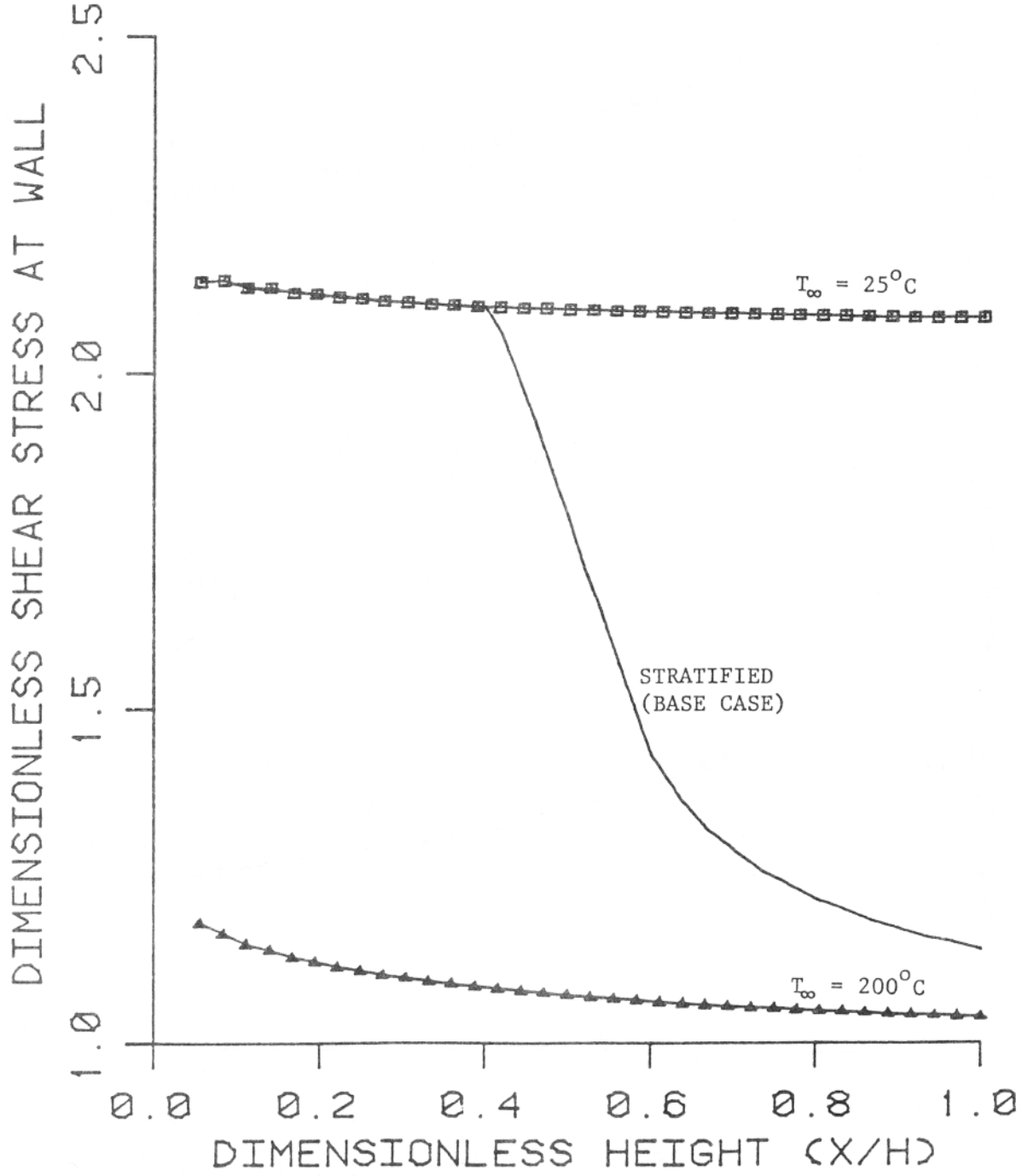

Figure 8 : Dimensionless wall shear against normalized height for the base case of stratified atmosphere and two other nonstratified cases.

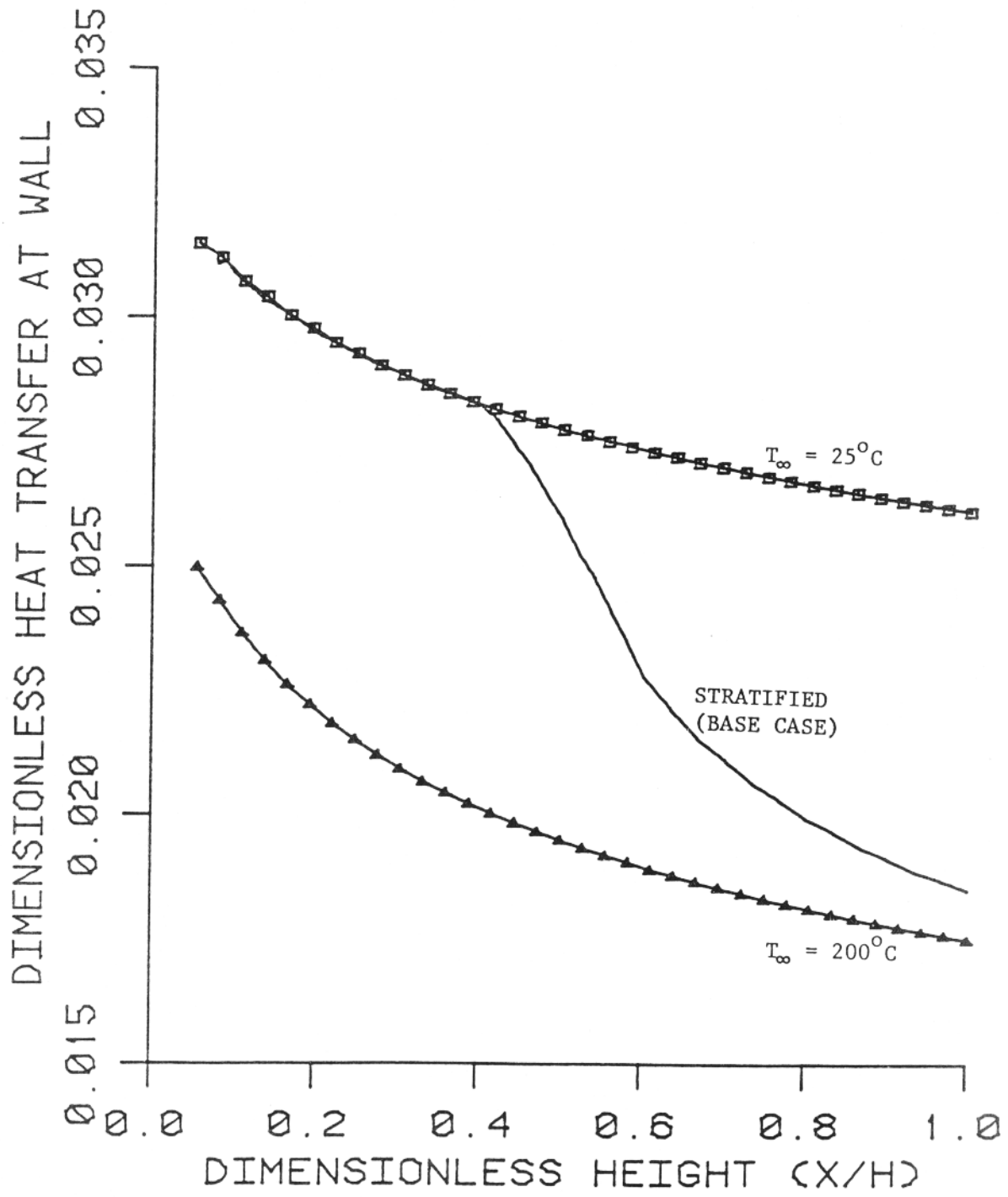

Figure 9 ; Dimensionless convective heat transfer to the wall against normalized height for the base case of stratified atmosphere and two other nonstratified cases.

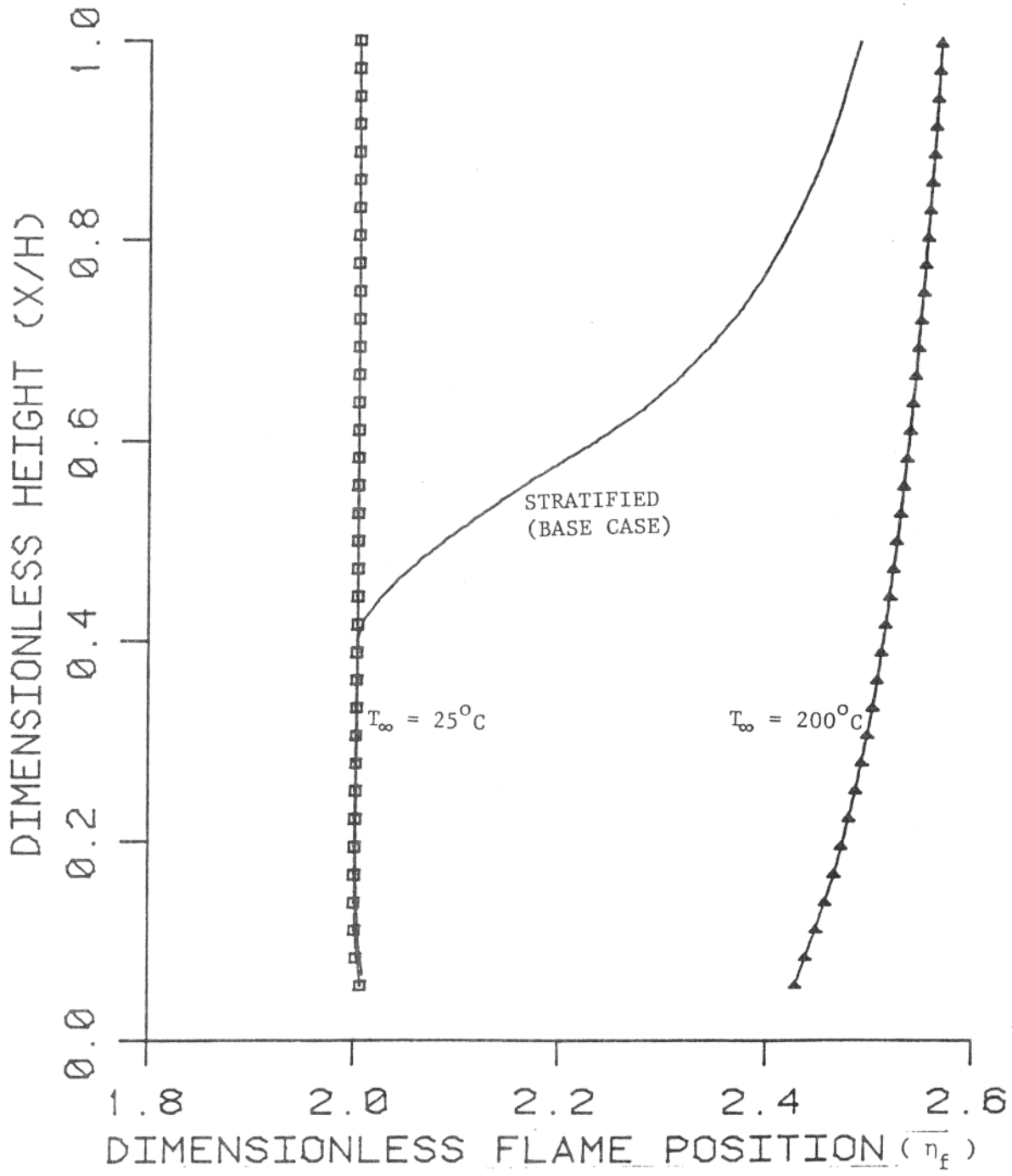

Figure 10 : Dimensionless flame stand-off distance against normalized height for the base case of stratified atmosphere and two other nonstratified cases.

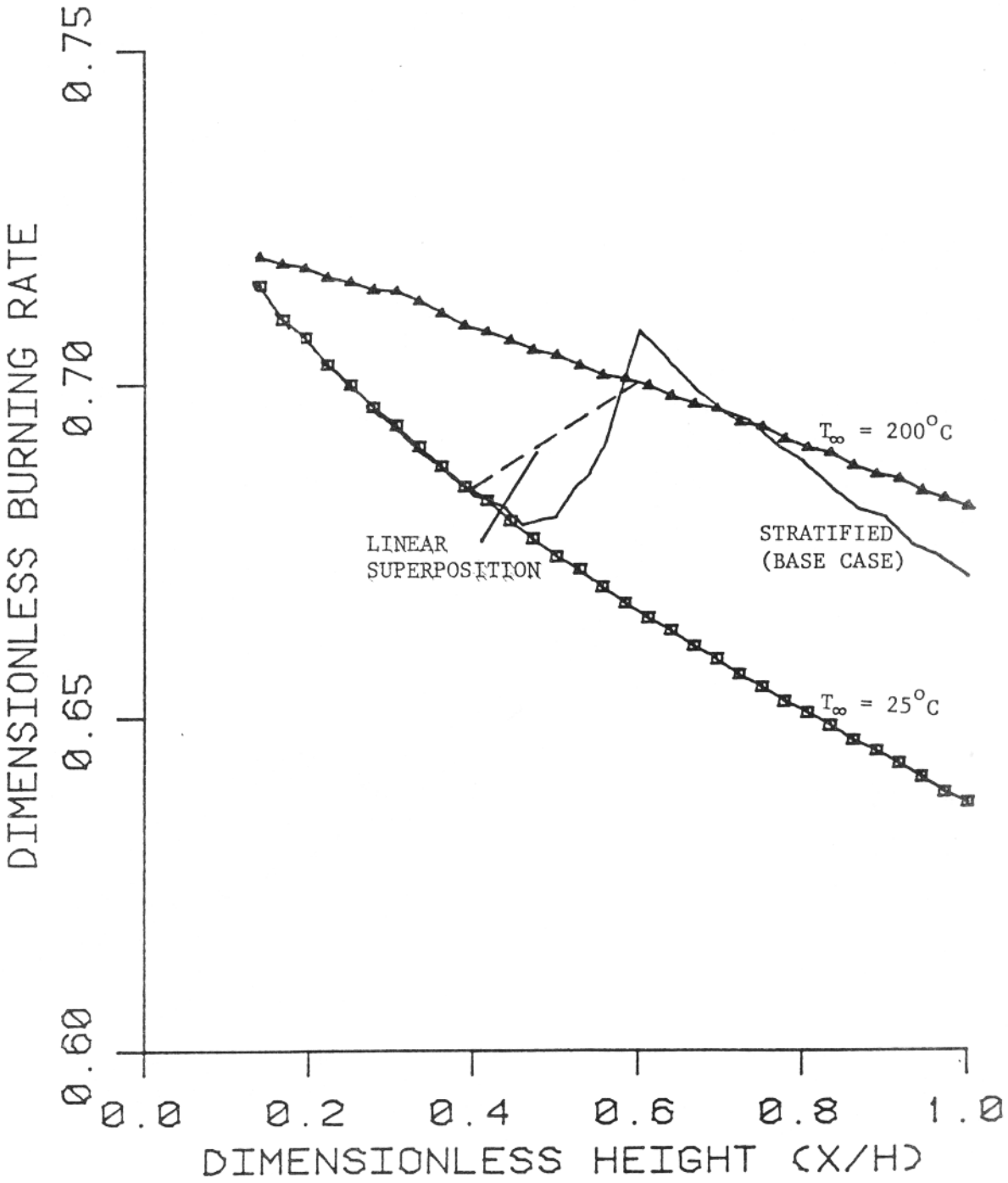

Figure 11 : Dimensionless burning rate against normalized height for the base case of stratified atmosphere and two other nonstratified cases.

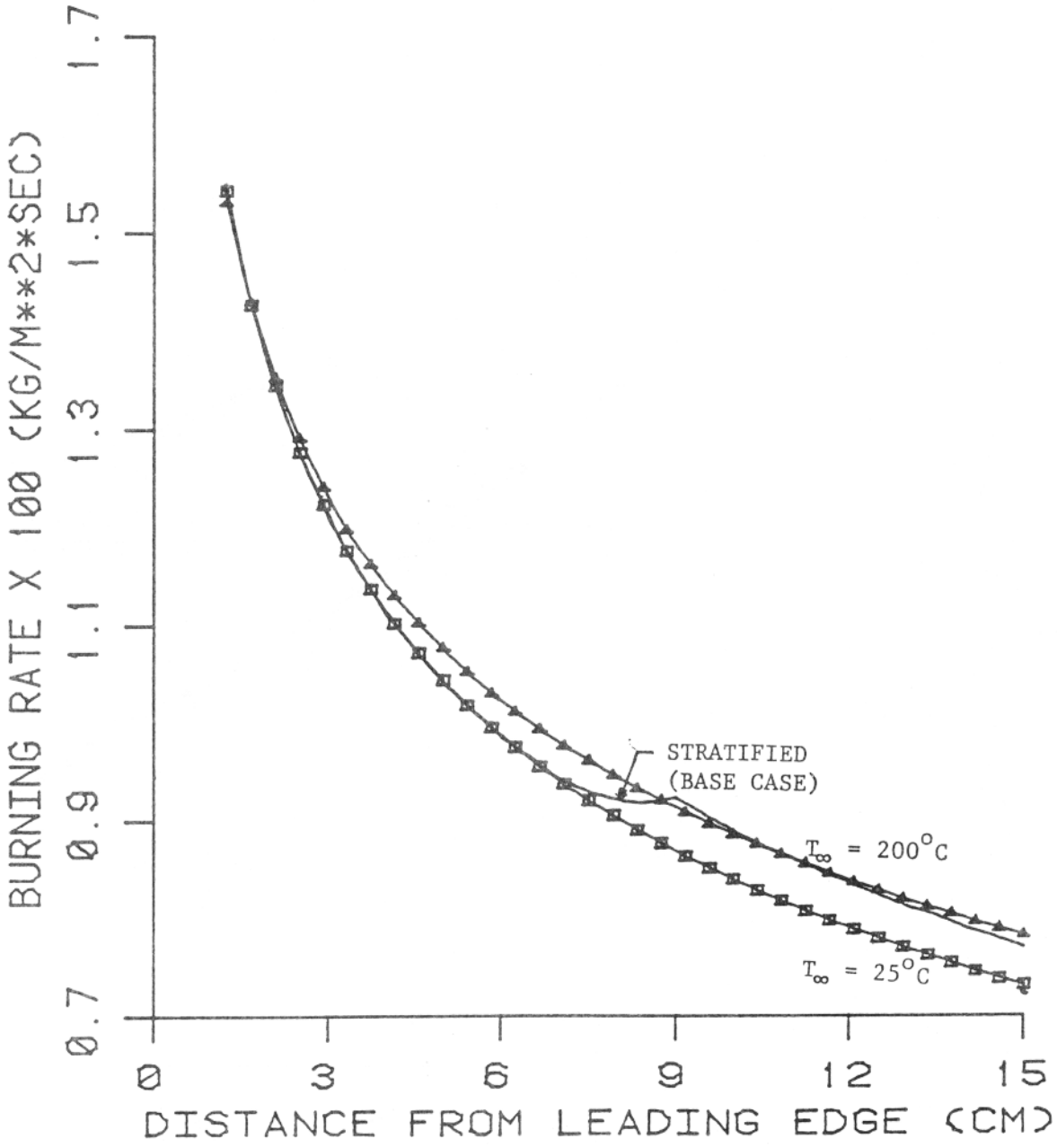

Figure 12 : Dimensional burning rate against distance from leading edge for the base case of stratified atmosphere and two other nonstratified cases.

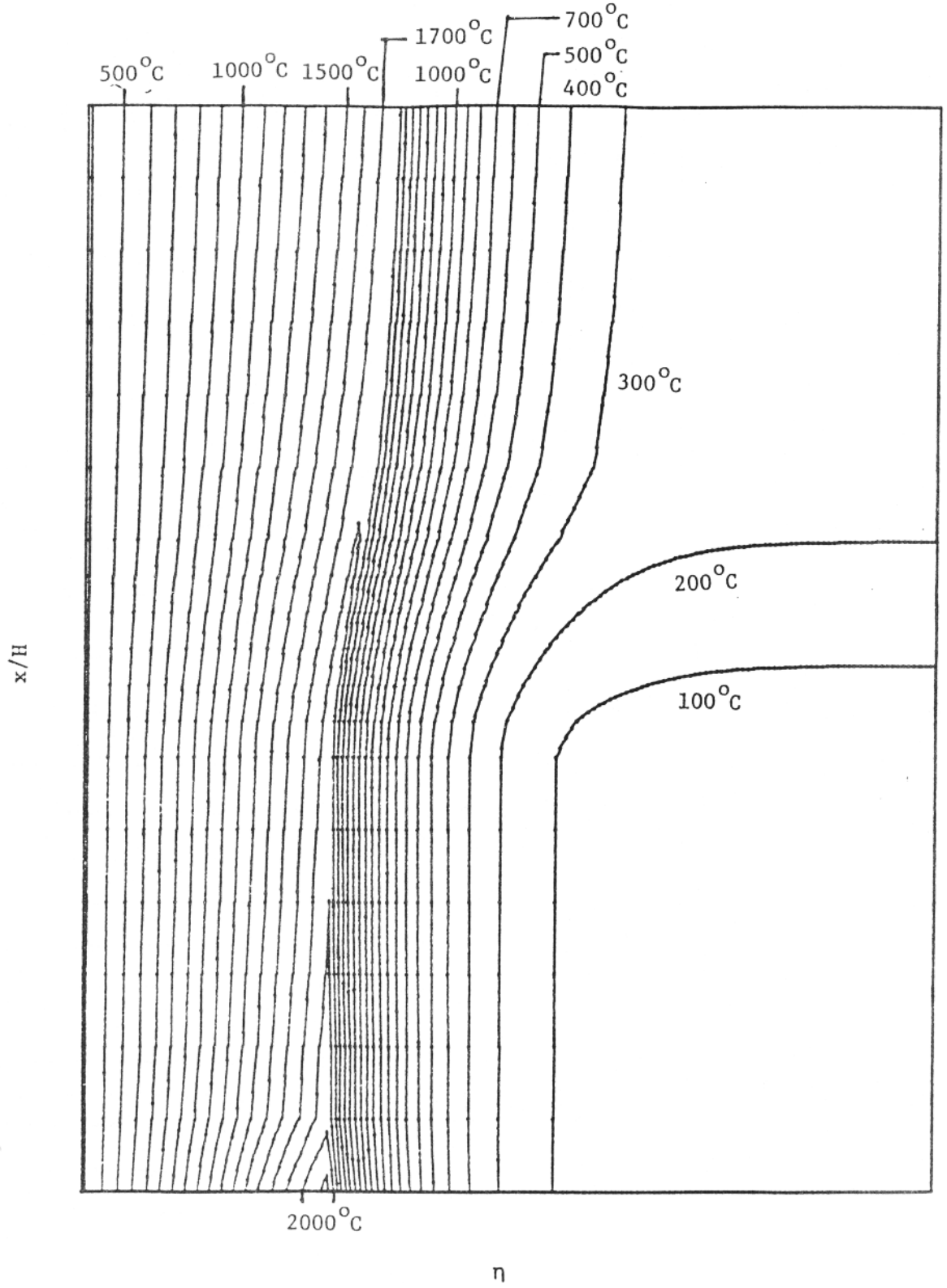

Figure 13 : Isothermal contours for the base case of stratified atmosphere for 100 degree steps.

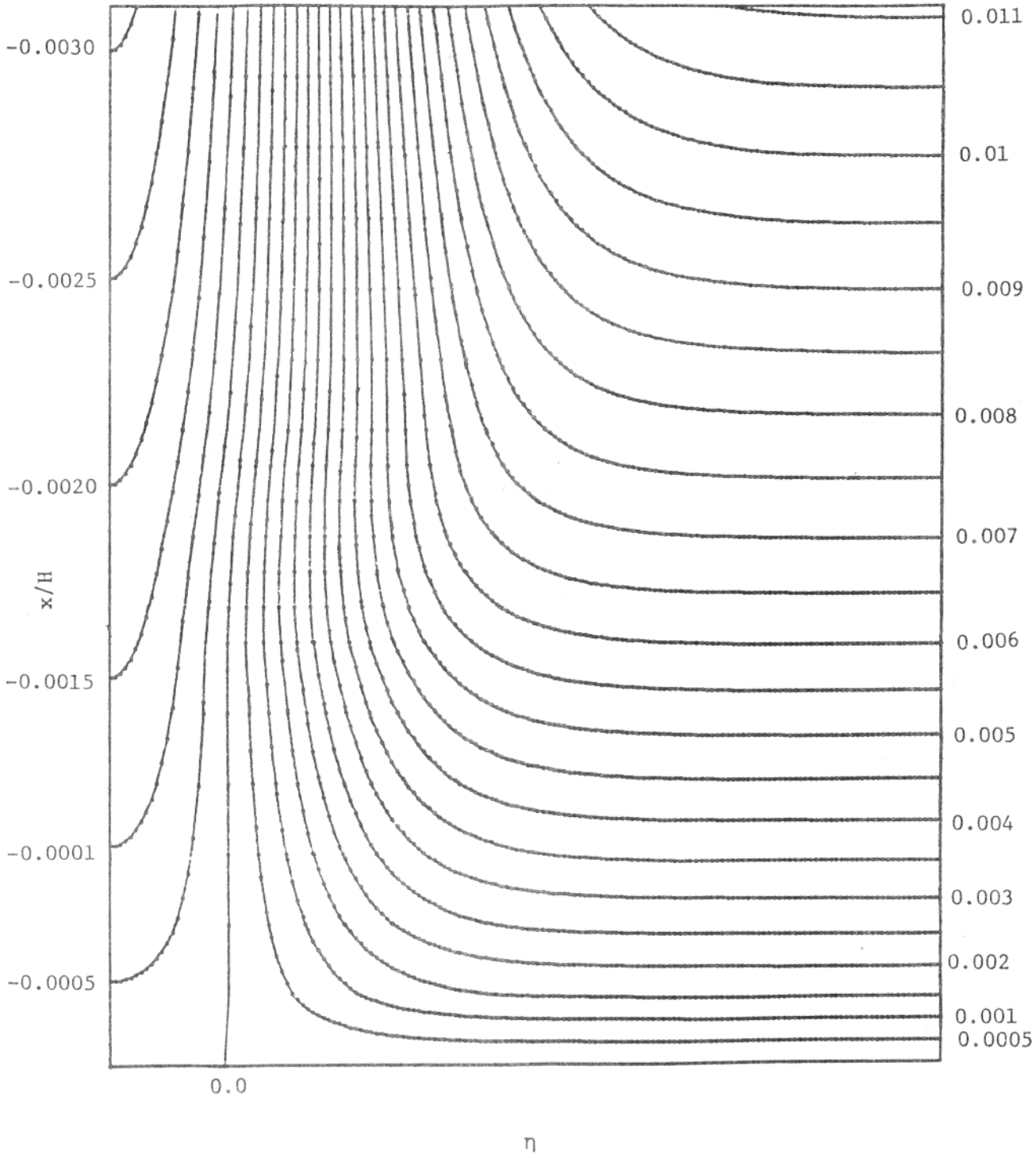

Figure 14 : Streamlines for the base case of stratified atmosphere ; values of ψ are specified.

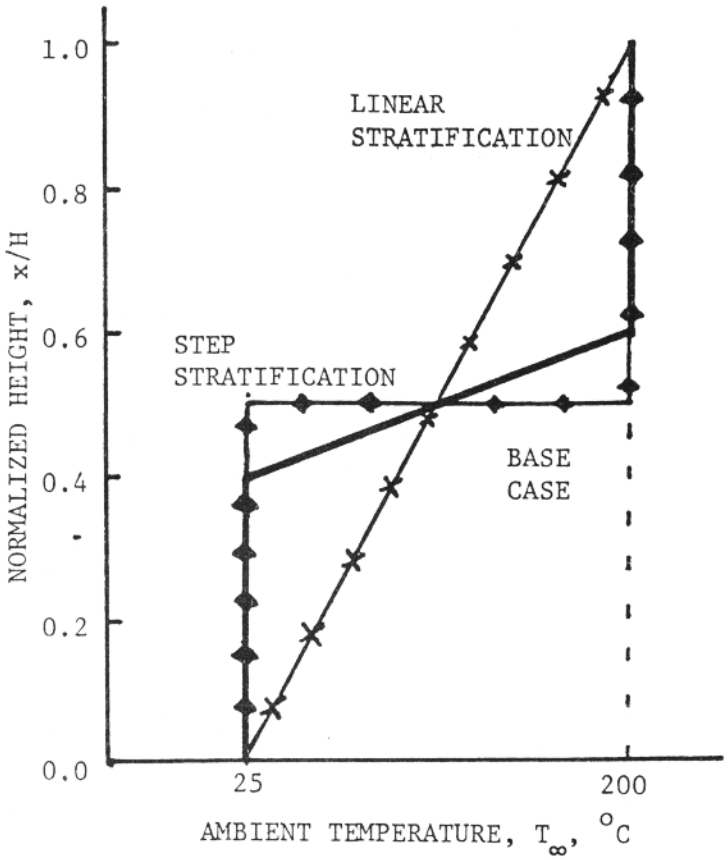

Figure 15: The base case (——) and two other cases of thermal stratification studied here are shown; step (—◆—) and linear (—×—) stratification.

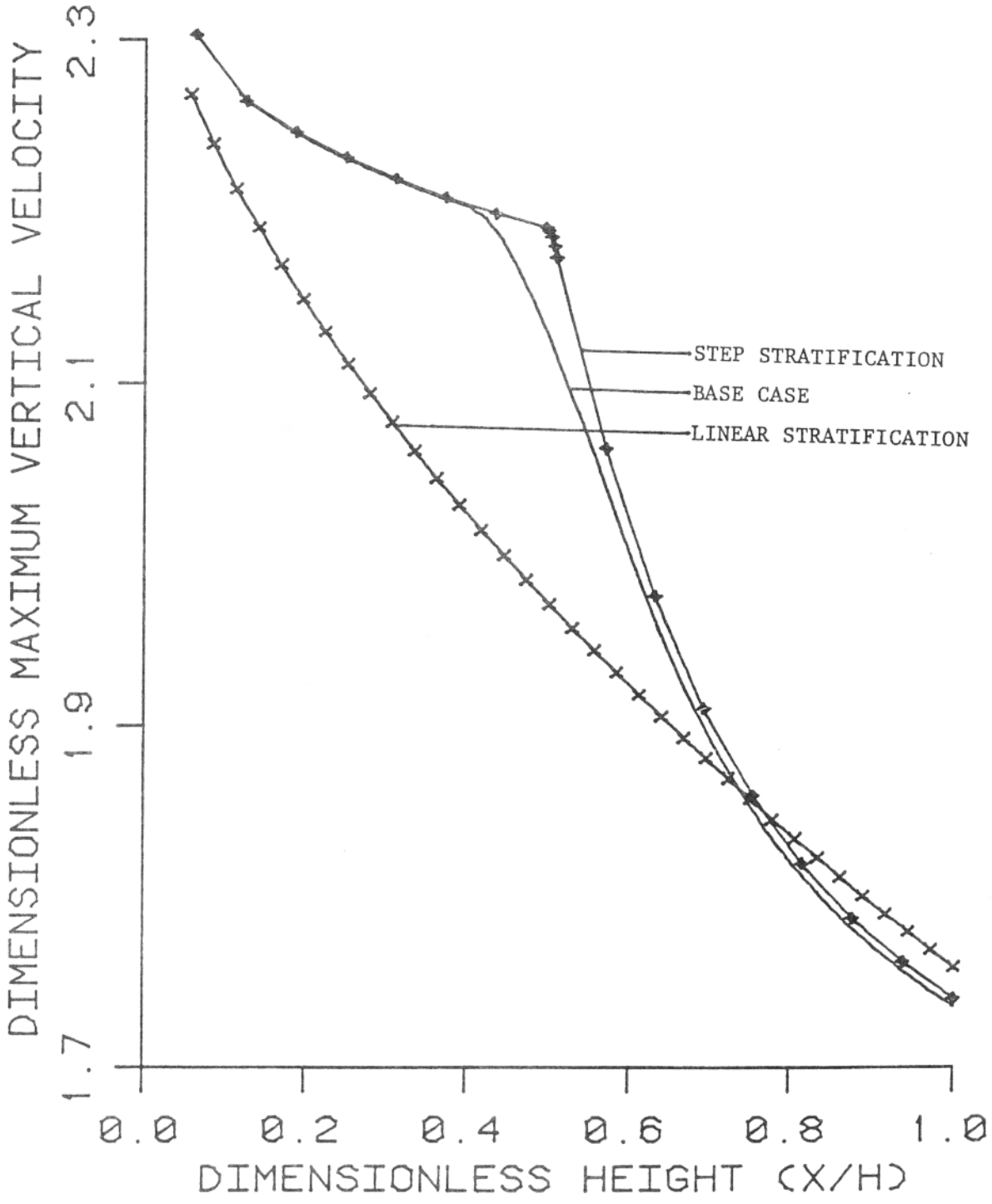

Figure 16 : Dimensionless maximum upward velocity against normalized height for three cases of stratification.

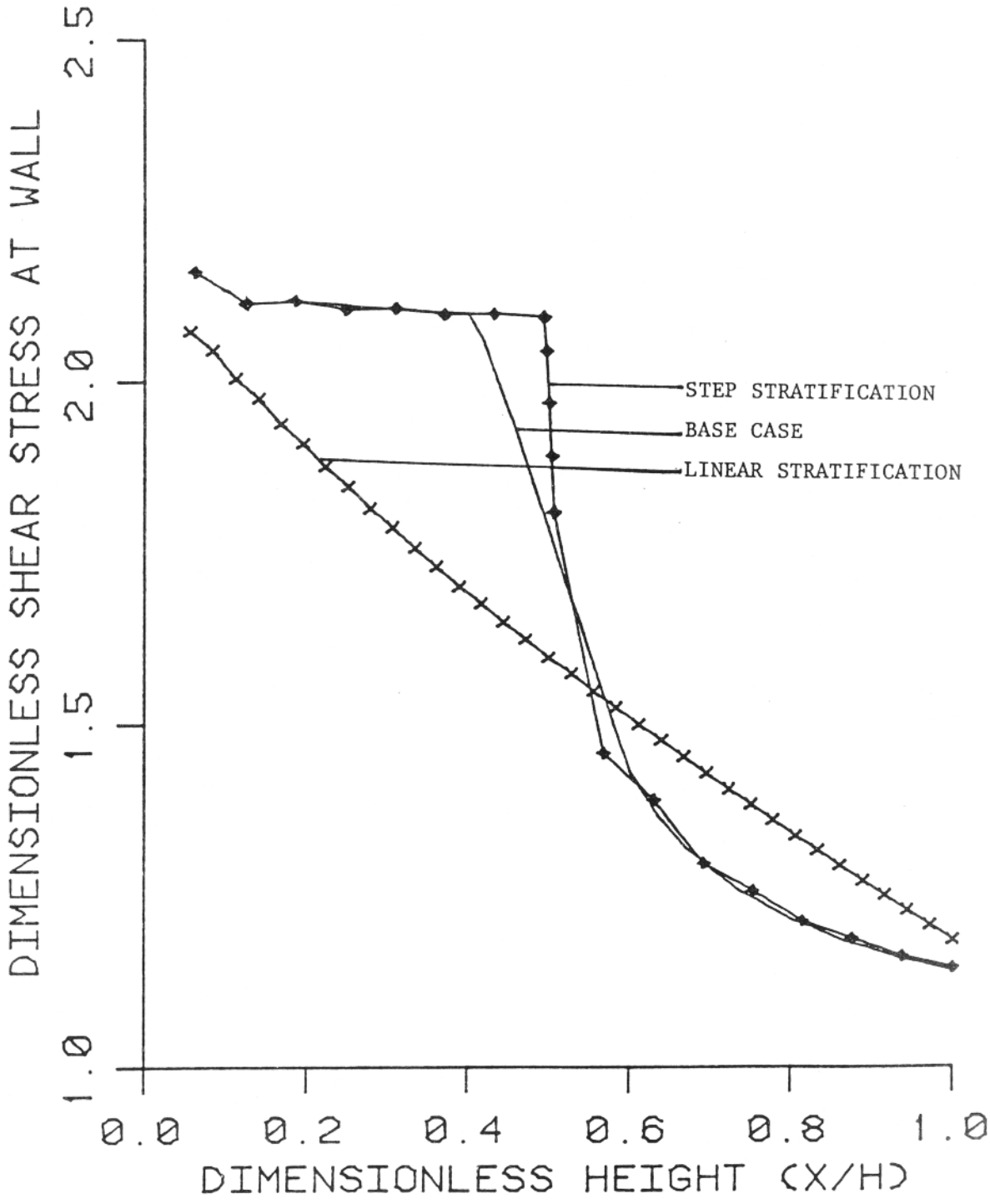

Figure 17 : Dimensionless wall shear against normalized height for three cases of stratification.

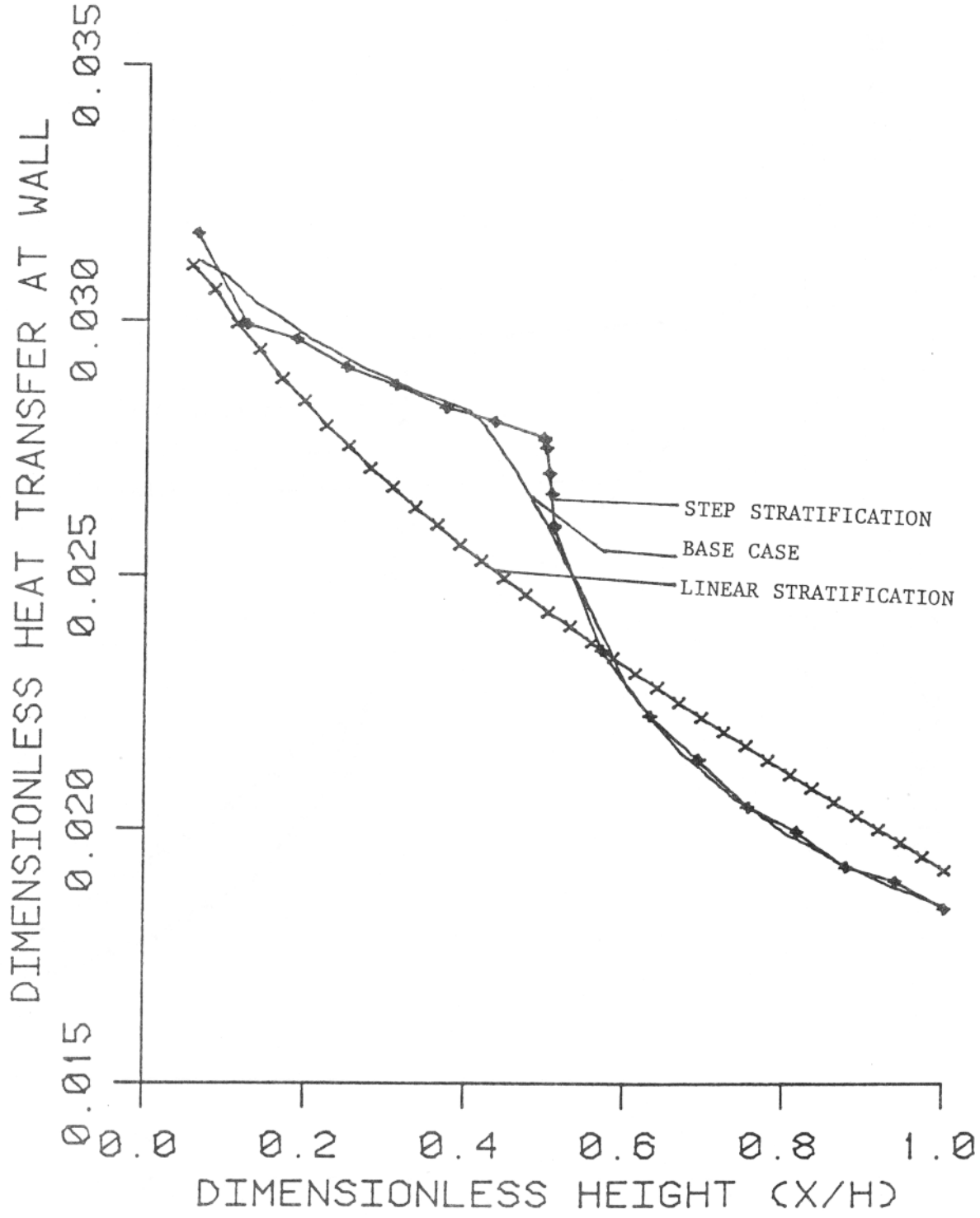

Figure 18 : Dimensionless convective heat transfer to the wall against normalized height for three cases of stratification.

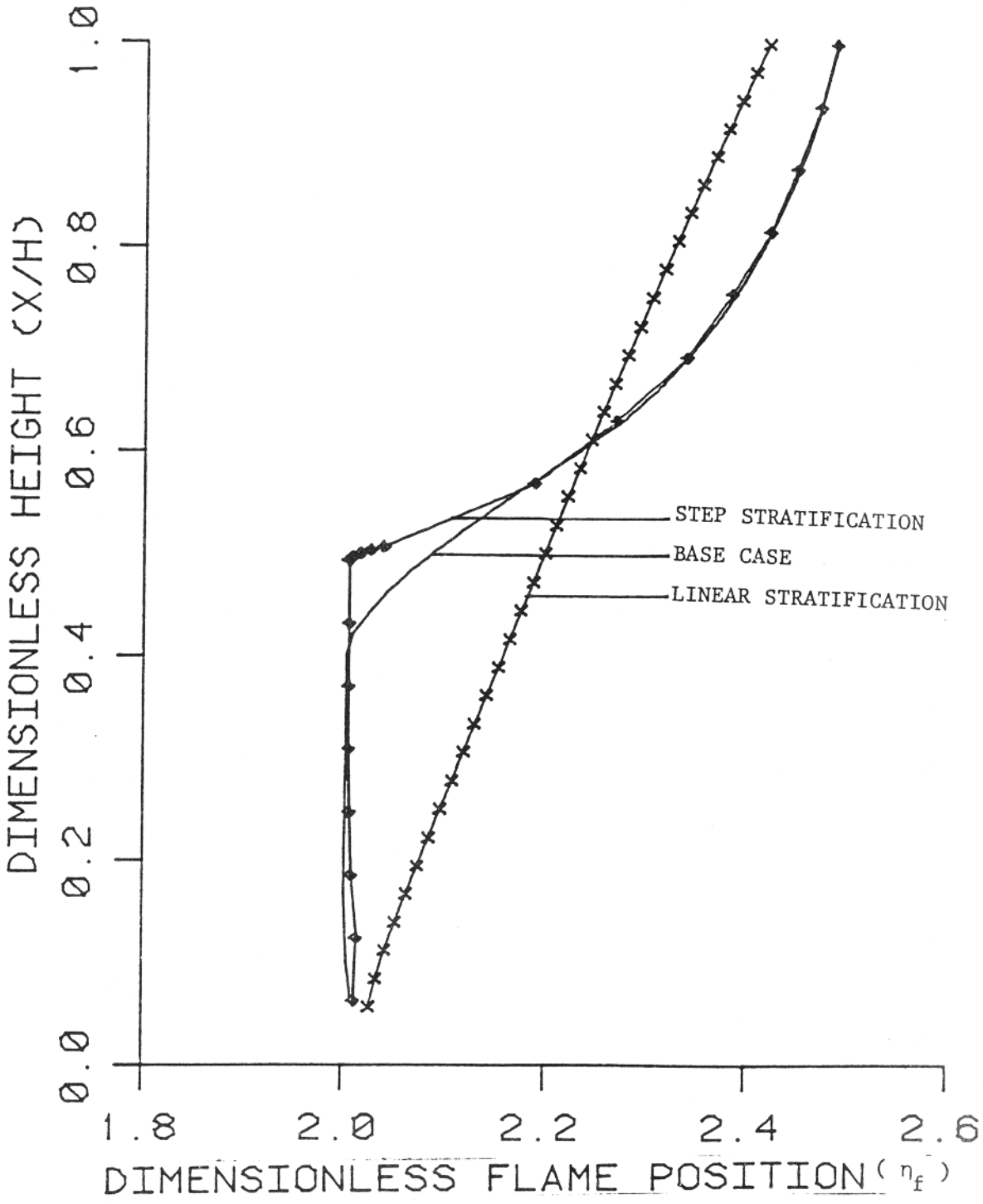

Figure 19 : Dimensionless flame stand-off distance against normalized height for three cases of stratification.

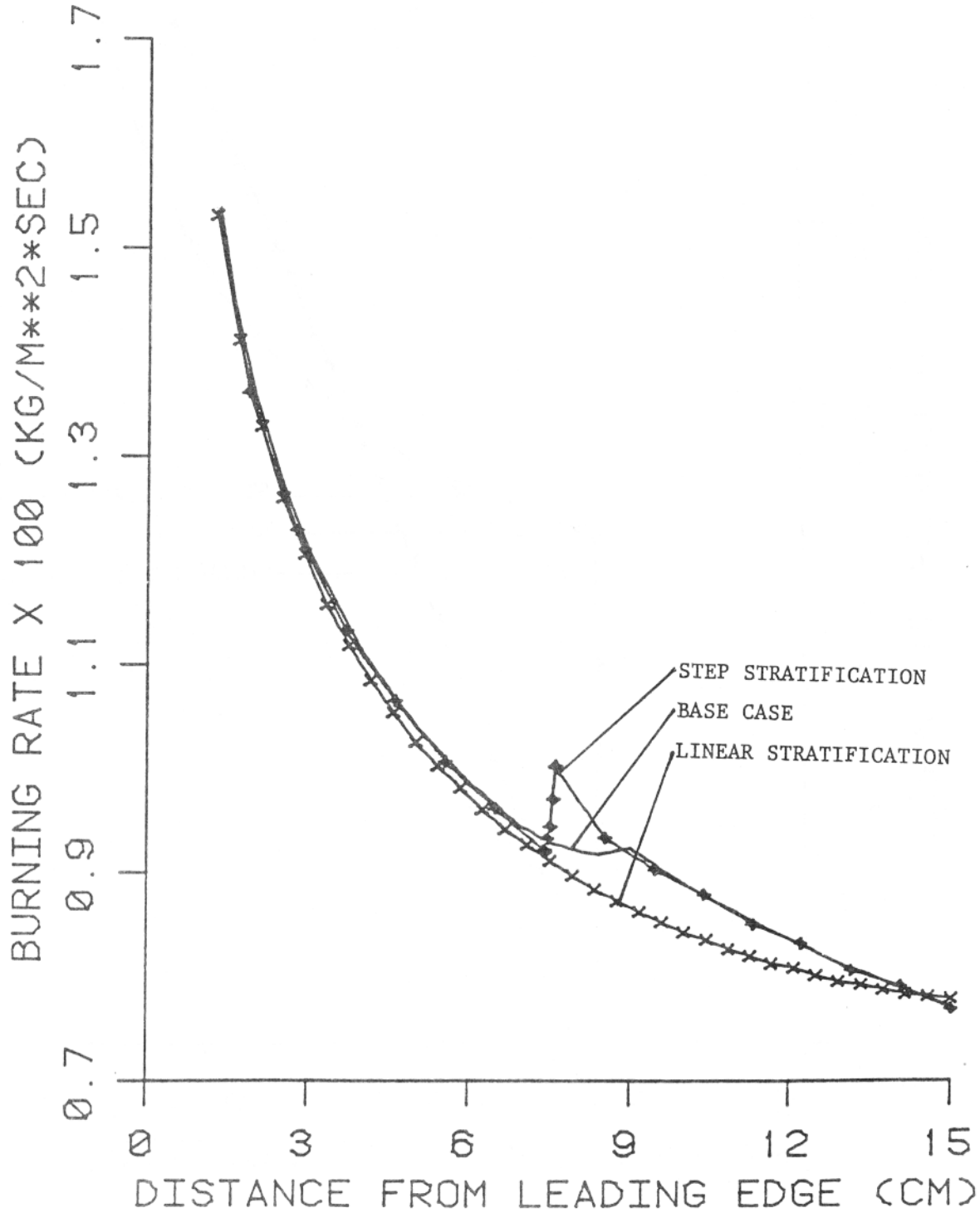

Figure 20 : Dimensional burning rate against distance from leading edge for three cases of stratification.

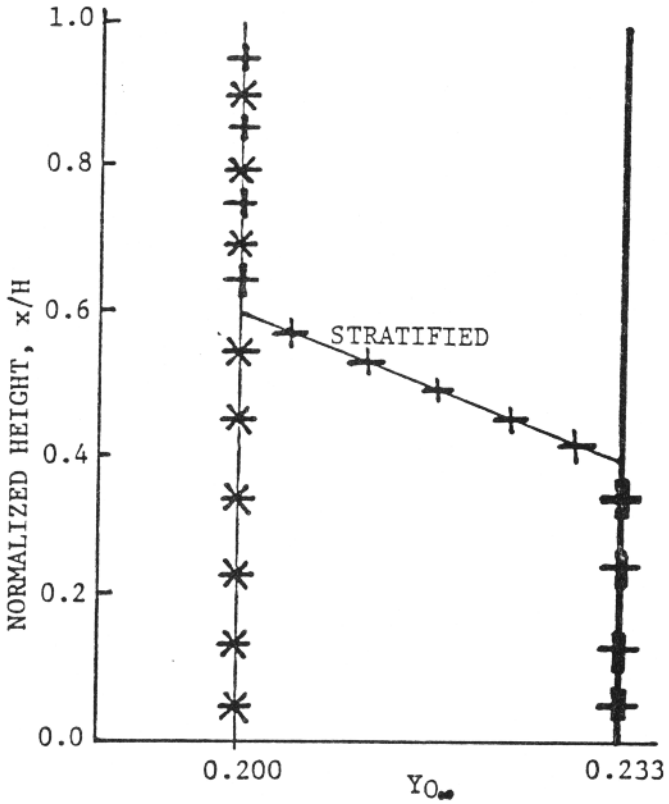

Figure 21 : Three cases for studying the effect of stratification in ambient oxidizer mass fraction: Y_O varying with height (—+—), Y_{O_∞} constant at 0.200 (—*—), and Y_{O_∞} constant at 0.233 (———). In all three cases a thermal stratification, same as that of the base case, is assumed.

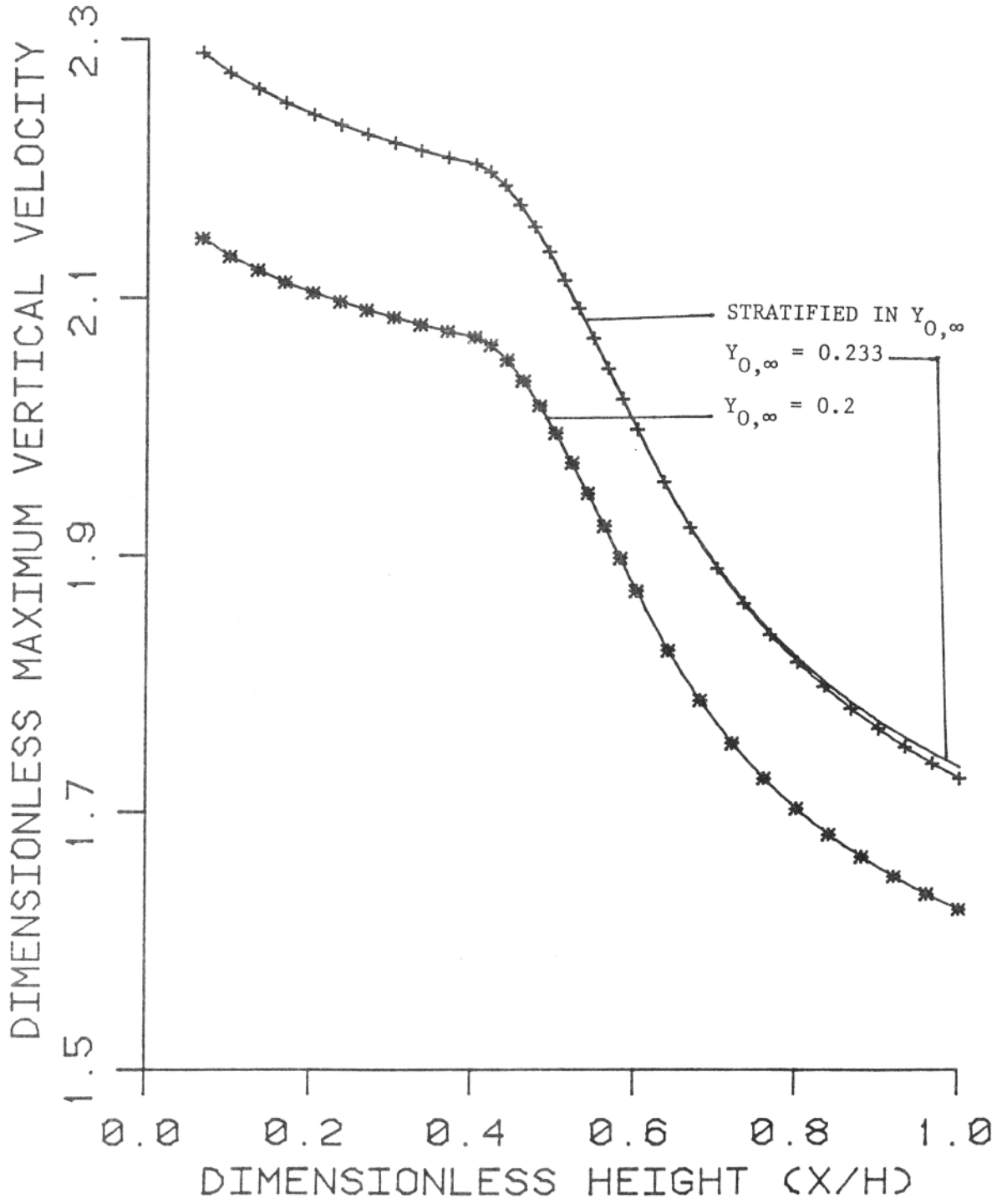

Figure 22 : Dimensionless maximum upward velocity against normalized height for the three cases indicated. (In all the cases shown, base thermal stratification is present.)

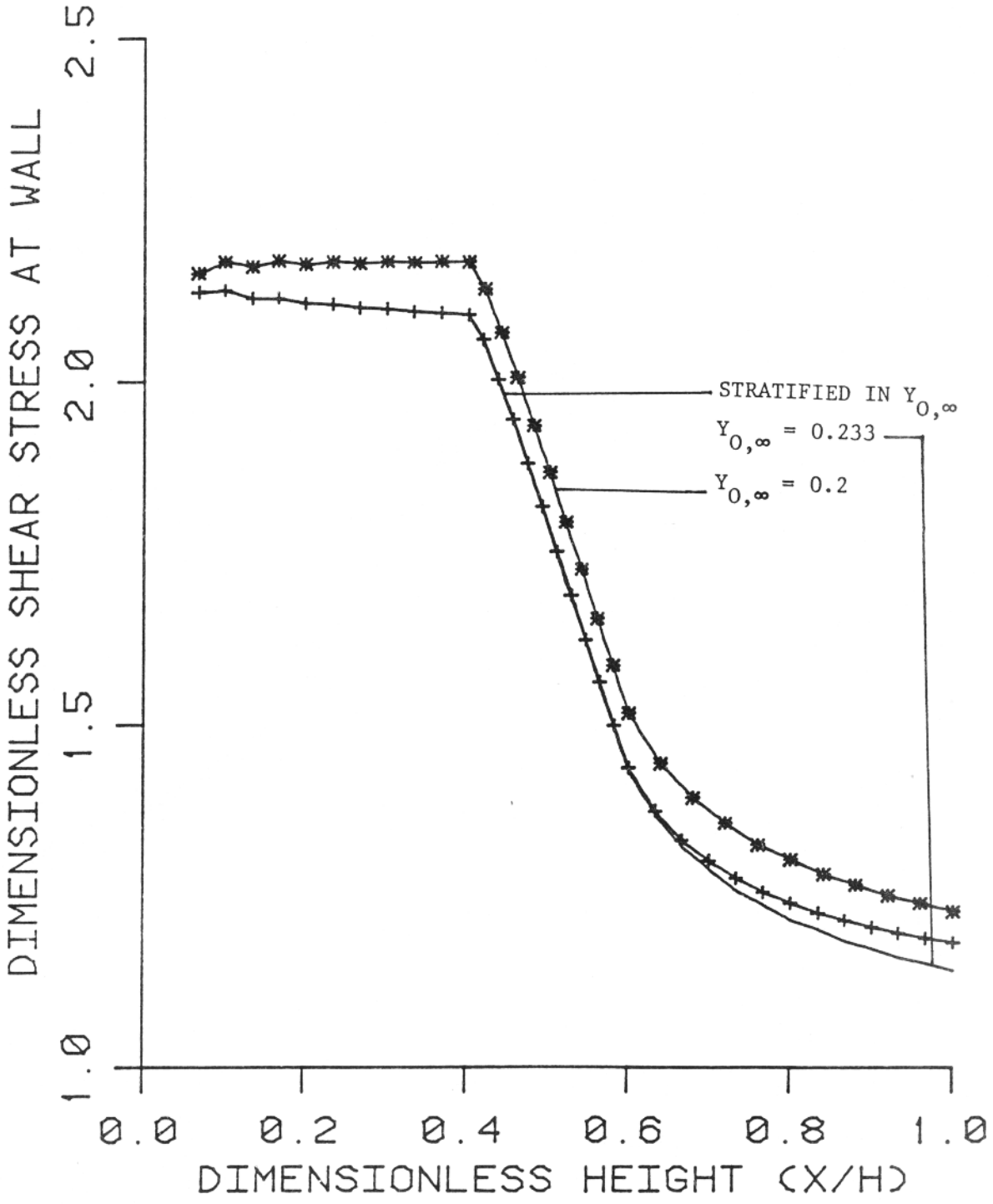

Figure 23 : Dimensionless wall shear against normalized height for the three cases indicated. (In all the cases shown, base thermal stratification is present.)

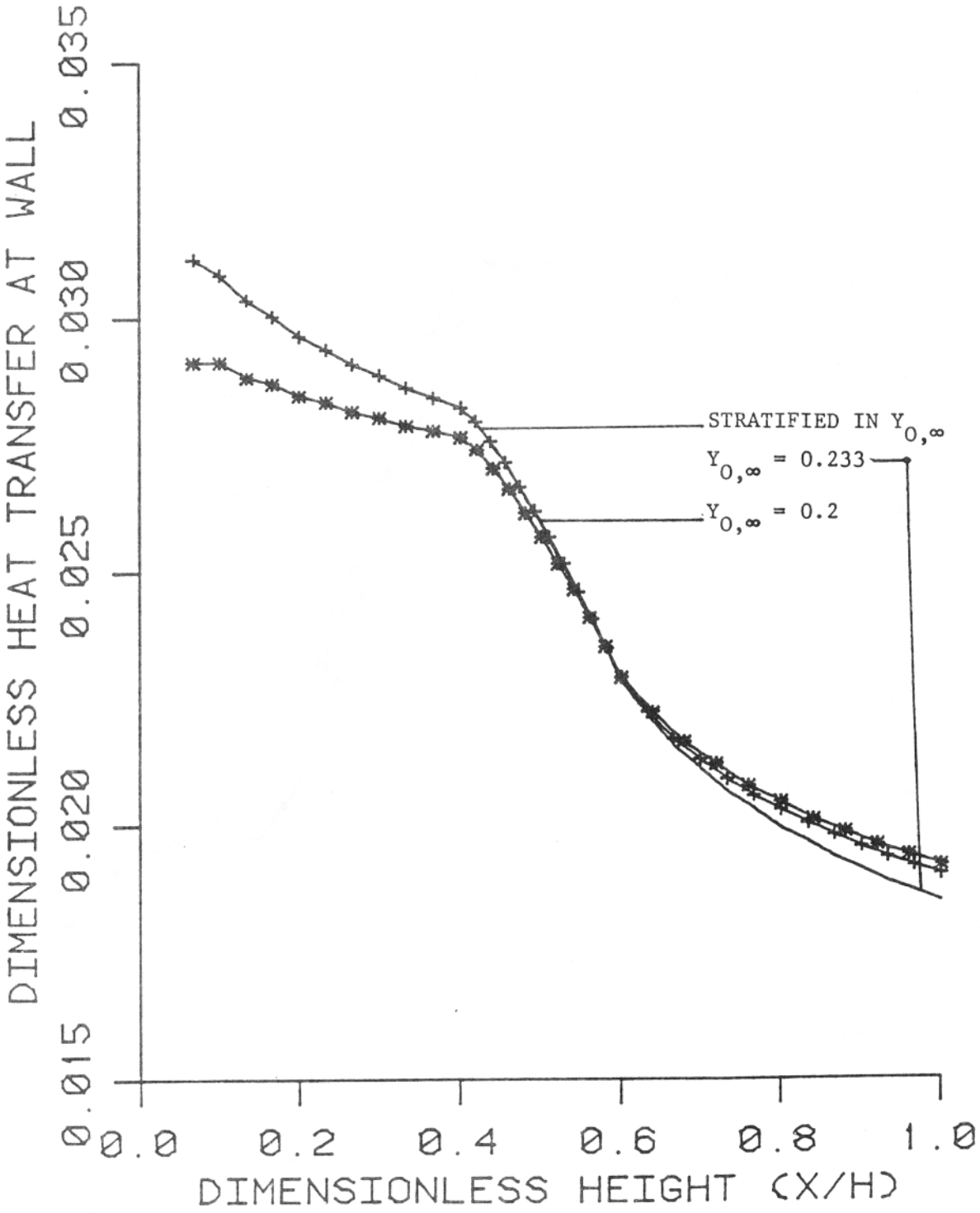

Figure 24 : Dimensionless convective heat transfer to the wall against normalized height for the three cases indicated. (In all the cases shown, base thermal stratification is present.)

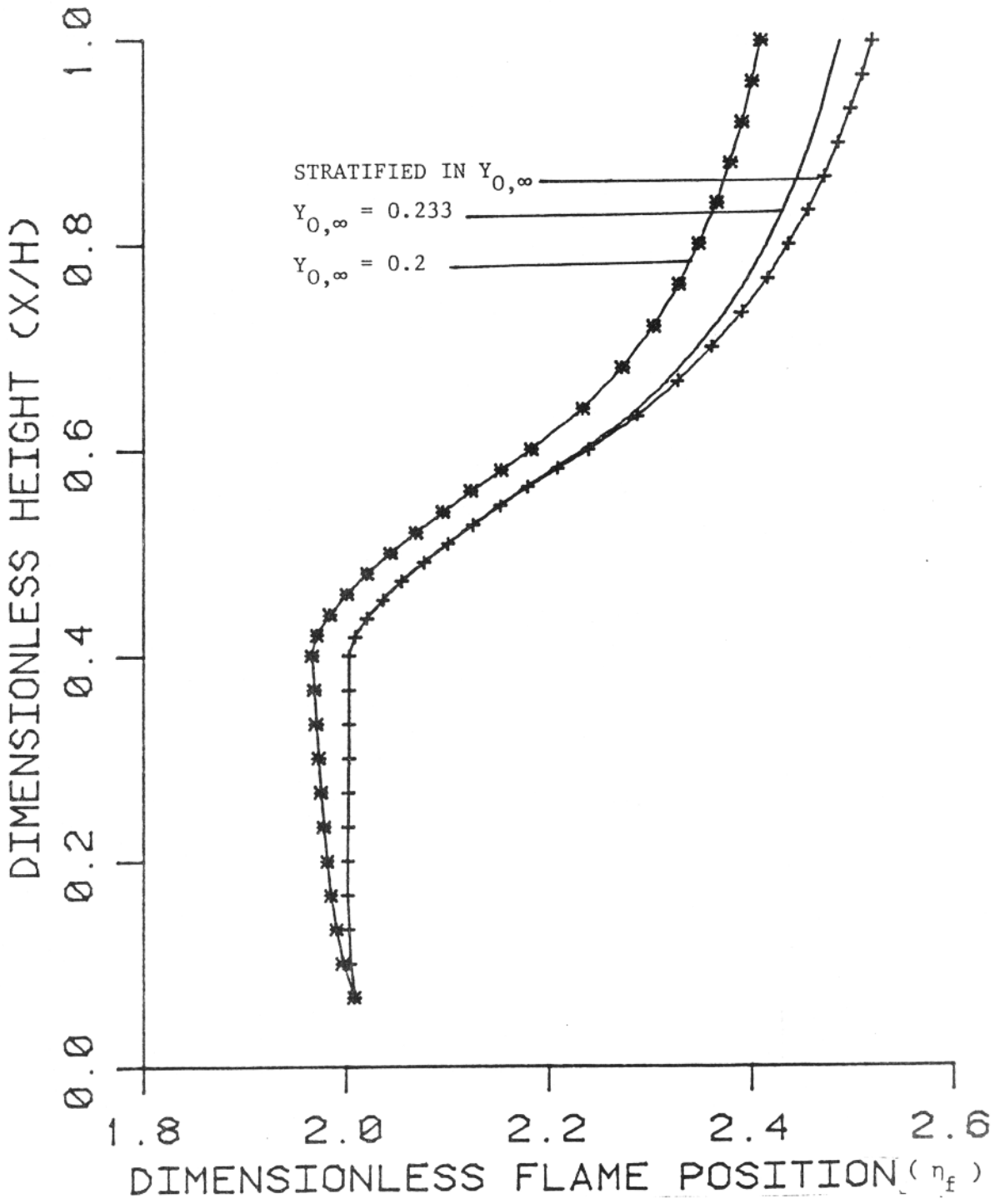

Figure 25 : Dimensionless flame stand-off distance against normalized height for the three cases indicated. (In all the cases shown, base thermal stratification is present.)

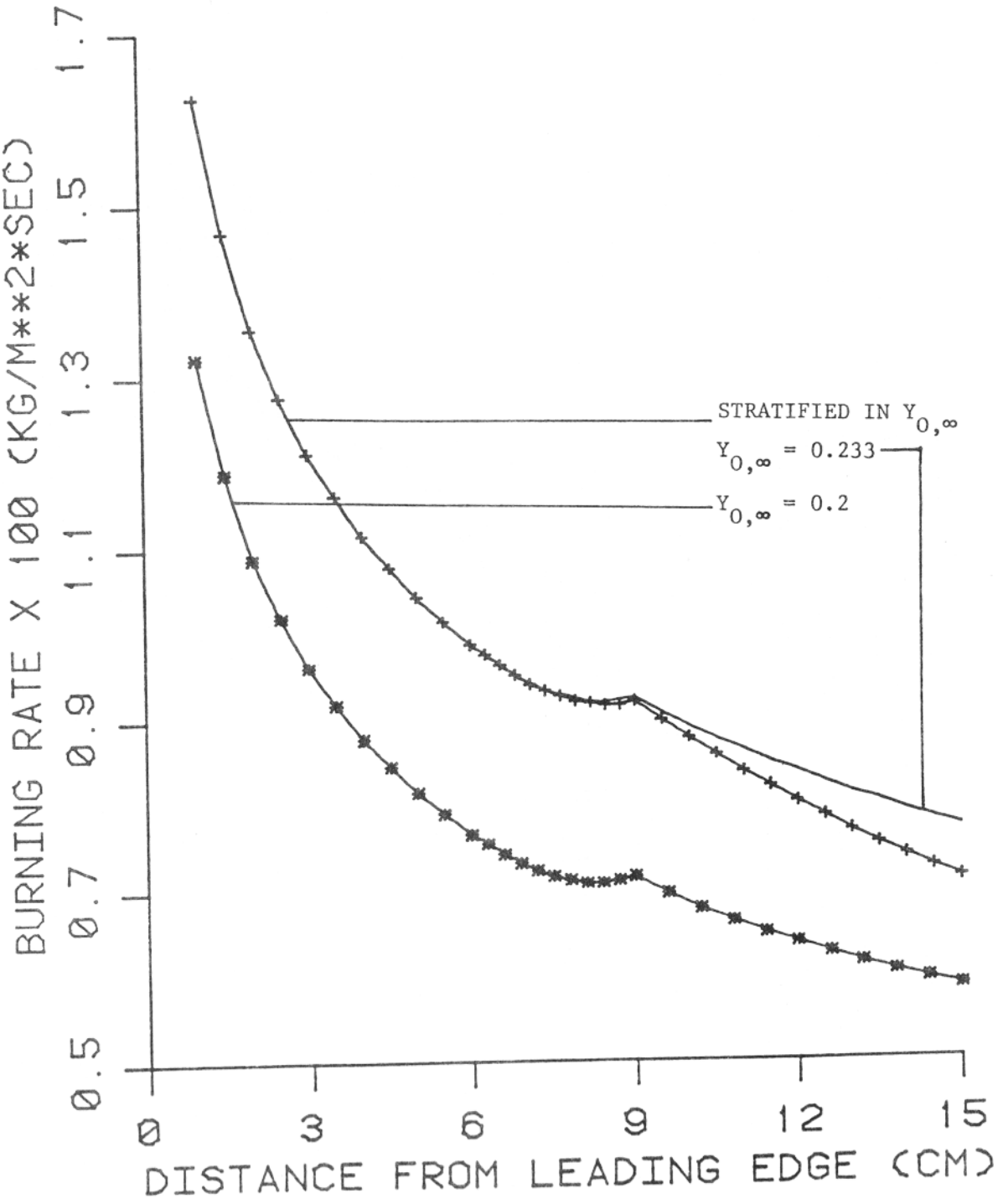

Figure 26 : Dimensional burning rate against distance from leading edge for the three cases indicated. (In all the cases shown, base thermal stratification is present.)

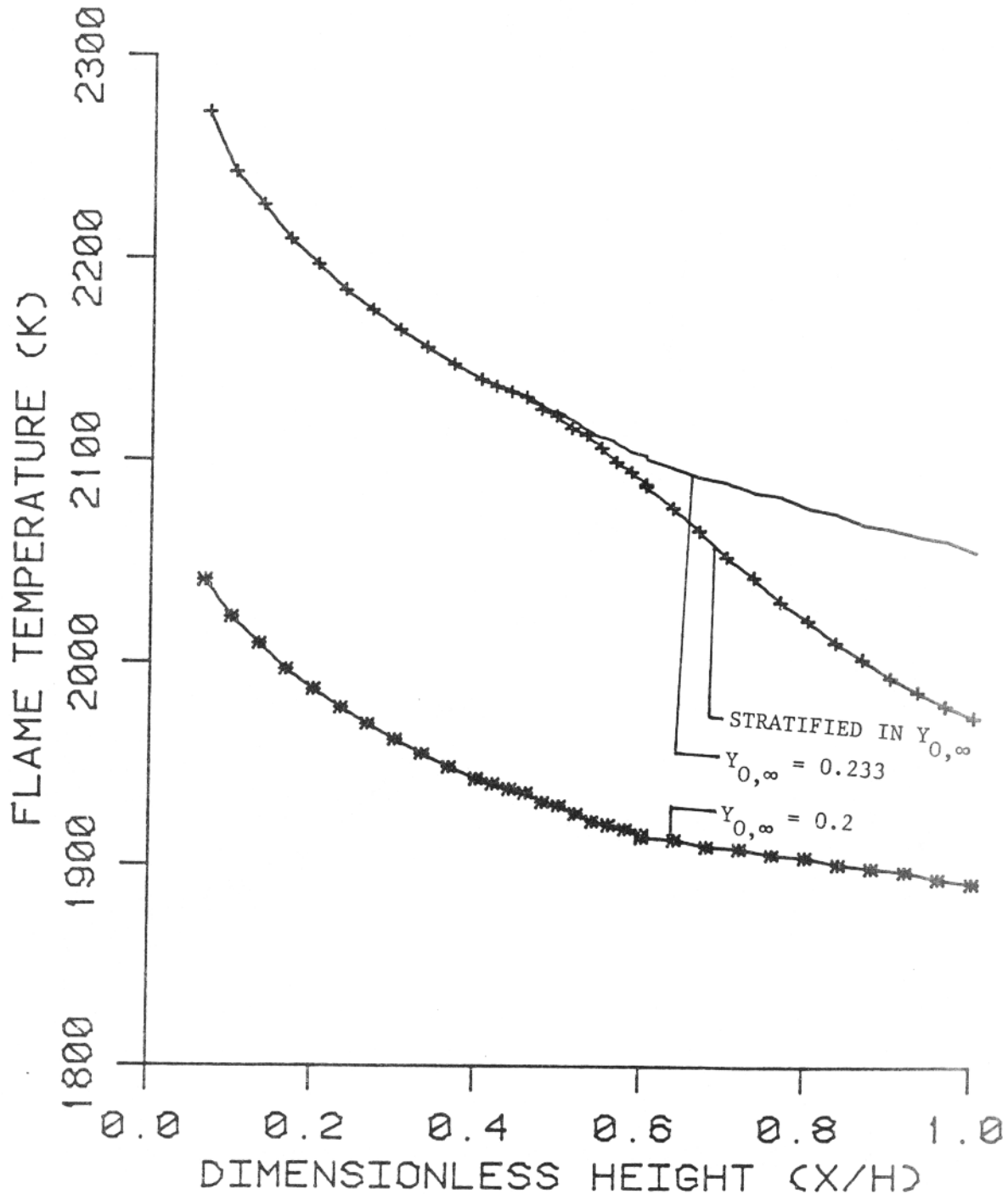

Figure 27 : Flame temperature against normalized height for the three cases indicated. (In all the cases shown, base thermal stratification is present.)

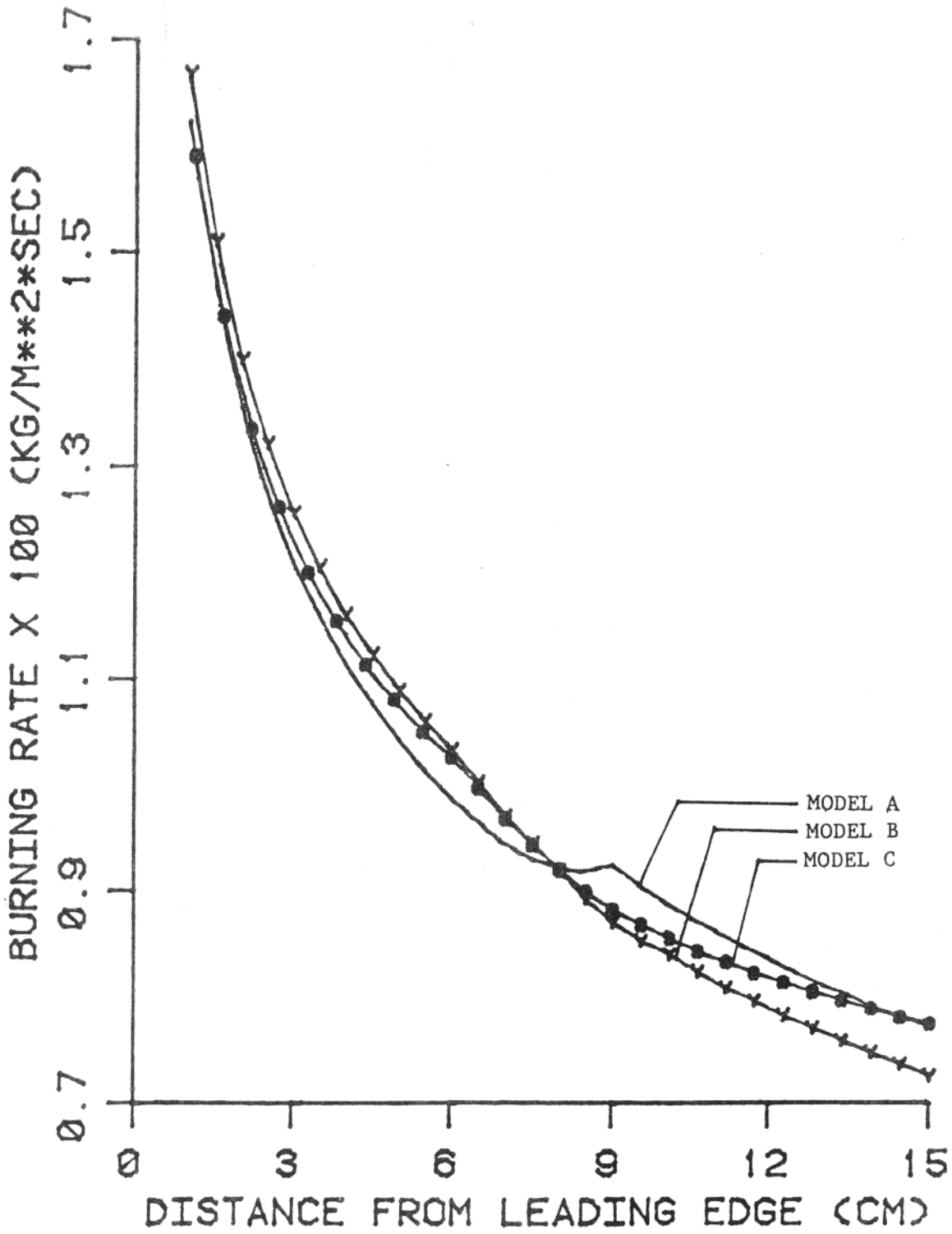

Figure 28 : Burning rate results using three different radiation models.

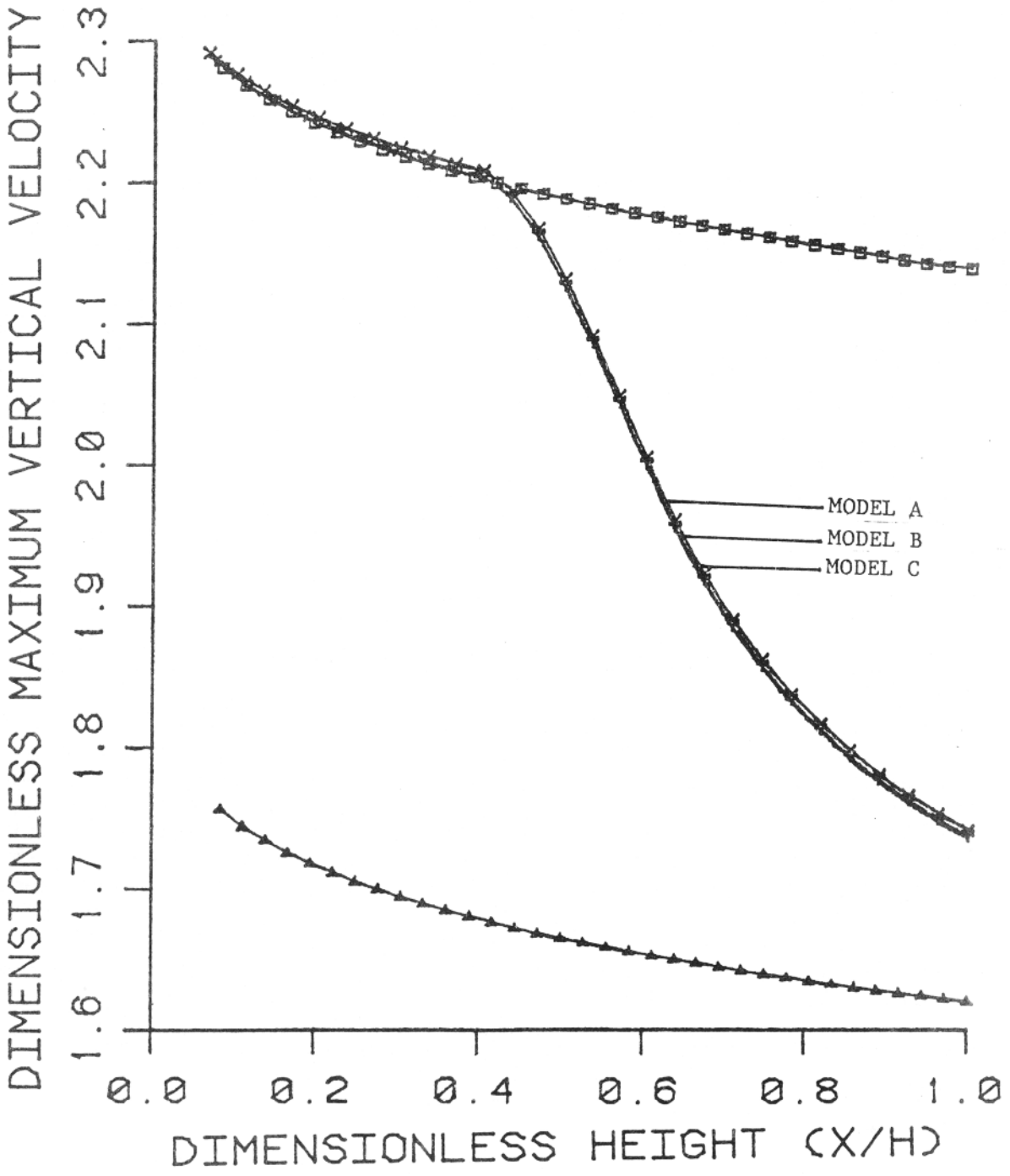

Figure 29 : Dimensionless maximum upward velocity results using three different radiation models.

NBS-114A (REV. 2-8C)

U.S. DEPT. OF COMM. BIBLIOGRAPHIC DATA SHEET (See instructions)	1. PUBLICATION OR REPORT NO. NBS/GCR-86/510	2. Performing Organ. Report No.	3. Publication Date March 1986

4. TITLE AND SUBTITLE

A Model for Vertical Wall Fire in a Stratified Atmosphere

5. AUTHOR(S)

Kulkarni, A.K., and Hwang, J.

6. PERFORMING ORGANIZATION (If joint or other than NBS, see instructions)

Department of Mechanical Engineering
The Pennsylvania State University
University Park, PA 16802

7. Contract/Grant No.

60NANB4D0037

8. Type of Report & Period Covered

Annual Report
8/15/84 to 8/14/85

9. SPONSORING ORGANIZATION NAME AND COMPLETE ADDRESS (Street, City, State, ZIP)

National Bureau of Standards
Department of Commerce
Gaithersburg, MD 20899

10. SUPPLEMENTARY NOTES

☐ Document describes a computer program; SF-185, FIPS Software Summary, is attached.

11. ABSTRACT (A 200-word or less factual summary of most significant information. If document includes a significant bibliography or literature survey, mention it here)

A comprehensive mathematical model is presented for understanding the characteristics of a burning vertical wall immersed in a quiescent ambient atmosphere having a nonuniform vertical distribution of temperature and oxidizer mass fraction. Such a stratified atmosphere occurs, for example, in the interior of a room or aircraft cabin on fire. A set of partial differential equations and suitable boundary conditions describing a laminar flow of exothermically reacting species is solved using the Keller Box finite difference scheme. Results of burning rate and flow parameters (such as the maximum vertical velocity, flame position, etc.) are presented for many different cases of stratified atmosphere. A comparison of these results with the results for the nonstratified atmosphere shows that the predicated burning rate for a thermally stratified case behaves like a linear combination of results for the corresponding nonstratified cases; however, this does not hold for compositionwise stratified atmosphere. The stratification has a substantial nonlinear effect on the flow structure in the wall fire. Different possibilities for surface reradiation models are also discussed.

12. KEY WORDS (Six to twelve entries; alphabetical order; capitalize only proper names; and separate key words by semicolons)

fire models; laminar burning; pyrolysis models; walls

13. AVAILABILITY

☒ Unlimited

☐ For Official Distribution. Do Not Release to NTIS

☐ Order From Superintendent of Documents, U.S. Government Printing Office, Washington, D.C. 20402.

☒ Order From National Technical Information Service (NTIS), Springfield, VA. 22161

14. NO. OF PRINTED PAGES

62

15. Price

$11.95

USCOMM-DC 6043-P80